British Journal of Pharmacology (2004) 142, 203–221
www.nature.com/bjp

EP_1- and FP-mediated cross-desensitization of the alpha (α) and beta (β) isoforms of the human thromboxane A_2 receptor

[1]Leanne P. Kelley-Hickie & *,[1]B. Therese Kinsella

[1]Department of Biochemistry, Conway Institute of Biomolecular and Biomedical Research, Merville House, University College Dublin, Belfield, Dublin 4, Ireland

1 Heterologous desensitization or intermolecular cross-talk plays a critical role in regulating intracellular signalling by diverse members of the G-protein-coupled receptor superfamily. We have previously established that the α and β isoforms of the human thromboxane A_2 receptor (TP) undergo differential desensitization of signalling in response to 17 phenyl trinor prostaglandin (PG)E_2, an agonist of the EP_1 subtype of the PGE_2 receptor (EP) family.

2 Herein, we investigated the molecular basis of TPα and TPβ desensitization in human embryonic kidney (HEK) 293 cells and in renal mesangial cells in response to 17 phenyl trinor PGE_2 and in response to the $PGF_{2\alpha}$ receptor (FP) agonist $PGF_{2\alpha}$, and sought to identify the target site(s) of those desensitizations.

3 Our results demonstrated that TPα and TPβ receptors are subject to desensitization in response to both EP_1 and FP receptor activation and that these effects are mediated by direct protein kinase (PK)C phosphorylation of the individual TP isoforms within their unique carboxyl-terminal (C)-tail domains.

4 Moreover, deletion/site-directed mutagenesis and metabolic labelling studies identified Thr^{337}, within TPα, and Thr^{399}, within TPβ, as the specific target residues for PKC phosphorylation and EP_1- and FP-mediated desensitization of TPα and TPβ signalling, respectively.

5 Hence, in conclusion, while the TPα and TPβ diverge within their C-tail domains, they have evolved to share a similar mechanism of PKC-induced phosphorylation and desensitization in response to EP_1 and FP receptor activation, though it occurs at sites unique to the individual TP isoforms.

British Journal of Pharmacology (2004) **142,** 203–221. doi:10.1038/sj.bjp.0705695

Keywords: Thromboxane receptor; 17 phenyl trinor prostaglandin E_2; prostaglandin $F_{2\alpha}$; desensitization; phosphorylation; phospholipase C; G-protein-coupled receptor

Abbreviations: C-tail, carboxyl-terminal tail; $[Ca^{2+}]_i$, intracellular calcium; EP, prostaglandin E_2 receptor; FP, prostaglandin $F_{2\alpha}$ receptor; GPCR, G-protein-coupled receptor; HA, haemagglutinin; HEK, human embryonic kidney; IP_3, inositol 1,4,5-trisphosphate; PAGE, polyacrylamide gel electrophoresis; PG, prostaglandin; PK, protein kinase; PL, phospholipase; PM, plasma membrane; TP, thromboxane A_2 receptor; TXA_2, thromboxane A_2

Introduction

The prostanoids consisting of the prostaglandins (PGs) and thromboxanes (TXs) act in an autocrine and paracrine manner to regulate diverse physiologic and pathophysiologic processes (Narumiya *et al*., 1999). The five primary prostanoids PGD_2, PGE_2, $PGF_{2\alpha}$, PGI_2 (prostacyclin) and TXA_2 signal through specific G-protein-coupled receptors (GPCRs) termed prostanoid-DP, EP (EP_1–EP_4), FP, IP and TP, respectively, and signal mainly through activation (DP, EP_2, EP_4, IP) or inhibition (EP_3) of adenylyl cyclase and through activation of phospholipase (PL)Cβ (EP_1, FP, TP) (Coleman *et al*., 1994; Narumiya *et al*., 1999). These autocoids mediate a variety of specific effects in diverse cell and tissue types, and depending on their actions on various types of smooth muscle (SM), such as vascular or bronchial SM, their receptors are further classified into the relaxant (DP, EP_2, EP_4, IP), contractile (EP_1, FP, TP) and inhibitory (EP_3) receptors (Narumiya *et al*., 1999).

The prostanoids may also influence neuronal activity, by either inhibiting or stimulating neurotransmitter release; they may modulate fever generation, pain perception, sleep induction, secretion and motility within the gastrointestinal tract, as well as the regulation of ion and water transport within the kidney (Narumiya *et al*., 1999). More specifically, $PGF_{2\alpha}$ regulates luteolysis of the corpus luteum in the estrous cycle (Narumiya *et al*., 1999), while TXA_2 and PGI_2 (prostacyclin) play a critical, dynamic role in vascular haemostasis, regulating platelet activation status and vascular tone (Armstrong, 1996; Wise & Jones, 1996; Narumiya *et al*., 1999). Hence, it is apparent that primary physiologic roles have been ascribed to many of the prostanoids and their receptors and those primary functions have been largely corroborated by observations from receptor knockout studies in mice (Narumiya *et al*., 1999; Sugimoto *et al*., 2000). However, the existence of overlapping ligand specificities and the co-existence of more than one prostanoid receptor type, subtype or isoform (Kiriyama *et al*., 1997; van der Vuurst *et al*., 1997; Fennekohl

*Author for correspondence; E-mail: Therese.Kinsella@UCD.IE
Advance online publication: 19 April 2004

et al., 1999) within a given cell/tissue adds greatly to the diversity of other actions of a given prostanoid within a particular cell or tissue type and greatly increases the complexity of downstream signalling resulting from prostanoid receptor activation (Narumiya *et al*., 1999). For example, the kidney is a major site of PG/TX synthesis (Breyer, 1998); while Northern blot analysis has confirmed the abundant co-expression of contractile EP_1, FP and TP receptors within the kidney (Sugimoto *et al*., 2000) and each of these receptors can mediate contraction of renal mesangial cells (Breyer, 1998), the relative roles of these individual prostanoids in renal function and the possibility of intermolecular cross-talk/counter-regulation of their responses remain to be investigated.

TXA_2 is a potent vasoconstrictor within the kidney, decreasing glomerular filtration rates (Wilkes *et al*., 1989; Spurney *et al*., 1993a, b; Breyer, 1998), and can greatly exacerbate renal dysfunction, such as the inflammatory condition glomerulonephritis (Badr, 1992; DeRubertis & Craven, 1993). In humans, TXA_2 signals through two TP receptor isoforms termed TPα and TPβ that arise through differential splicing and that are identical for their N-terminal 328 amino acids but differ within their carboxyl terminal (C)-tail domains (Hirata *et al*., 1991; Raychowdhury *et al*., 1994). Whereas the relevance of two receptors for TXA_2 in humans, but not in other species thus far investigated, is unknown, there is substantial evidence that they exhibit critical differences in signalling and patterns of expression (Miggin & Kinsella, 1998; Coyle *et al*., 2002) and therefore it is likely that TPα and TPβ have distinct physiologic/pathophysiologic roles (Kinsella, 2001). While both TPα and TPβ mediate identical ligand binding and Gq-dependent activation of PLCβ, their primary effector (Raychowdhury *et al*., 1994; Habib *et al*., 1997; Walsh *et al*., 1998; Walsh M. *et al*., 2000; Kinsella, 2001), they oppositely regulate adenylyl cyclase activity (Hirata *et al*., 1996) and TPα, but not TPβ, mediates activation of the novel G protein/tissue transglutaminase Gh (Vezza *et al*., 1999). Additionally, while both TPs undergo agonist-induced phosphorylation (Habib *et al*., 1997; 1999), TPβ, but not TPα, is subject to internalization and downregulation following prolonged exposure to the TXA_2 mimetic U46619 (Parent *et al*., 1999; 2001). In studies investigating cross-talk between TXA_2 and other prostanoids, it was established that signalling by TPα, but not TPβ, is subject to prostacyclin and PGD_2-mediated desensitization and inhibition of signalling, involving direct protein kinase (PK) A phosphorylation of TPα within its unique C-tail domain (Walsh M.T. *et al*., 2000; Foley *et al*., 2001). Moreover, consistent with the latter, it is now evident that TPα, but not the TPβ, is a target for nitric oxide-induced desensitization that occurs through a PKG mechanism involving direct phosphorylation of TPα at S^{331} within its unique C-tail domain (Reid & Kinsella, 2003). These latter studies point to an essential role for TPα in vascular haemostasis and point to a redundant or an, as yet, unidentified role for TPβ in this essential physiologic process (Walsh M. *et al*., 2000; Foley *et al*., 2001; Reid & Kinsella, 2003). In other studies investigating possible cross-talk between the TP isoforms and the contractile EP_1 receptor, it was established that TPα and TPβ are also subject to differential desensitization or inhibition of signalling in response to the EP_1 agonist 17 phenyl trinor PGE_2 (Walsh & Kinsella, 2000). While EP_1-mediated desensitization of both TPα and TPβ signalling occurred through a GF 109302X sensitive, H-89-insensitive mechanism, implying an involvement of PKC (Walsh & Kinsella, 2000), the precise mechanism of EP_1-mediated TPα/TPβ desensitization remains to be investigated.

Thus, in the current study, we sought to investigate the molecular basis of the differential sensitivities of TPα *versus* TPβ to EP_1-mediated desensitization and to identify those residues/sites within TPα and TPβ specifically targeted by EP_1 signalling. Moreover, since FP receptors are abundantly co-expressed along with the TPs and EP_1 receptors, such as in the kidney where they bring about contraction of renal mesangial cells (Watabe *et al*., 1993; Abramovitz *et al*., 1994; Breyer, 1998; Sugimoto *et al*., 2000), we sought to investigate the intermolecular cross-talk mediated by the EP_1 and FP receptor agonists 17 phenyl trinor PGE_2 and $PGF_{2\alpha}$ on TP signalling within primary human mesangial cells (1° hMCs), comparing it to that which occurs to the individual TPα and TPβ receptors stably overexpressed in human embryonic kidney (HEK) 293 cells. Our results demonstrated that TPα and TPβ receptors are subject to desensitization in response to both EP_1 and FP receptor activation and that these effects are mediated by direct PKC phosphorylation at sites unique to the individual TP receptors, whereby Thr^{337} and Thr^{399} have been identified as the specific phospho-target residues within TPα and TPβ, respectively.

Experimental procedures

Materials

17 phenyl trinor PGE_2, SC-19220, Misoprostol, U46619 and [^{3}H]SQ29,548 were obtained from the Cayman Chemical Company, Ann Arbor, MI, U.S.A. $PGF_{2\alpha}$ and Tri Reagent™ were obtained from Sigma, Saint Louis, MO, U.S.A. FURA2/AM, D-myo-inositol 1,4,5-trisphosphate, 3-deoxyhexasodium salt was from Calbiochem, Darmstadt, Germany. [^{32}P]orthophosphate (8000–9000 Ci mmol^{-1}) was from DuPont NEN, Boston, MA, U.S.A. [^{3}H]IP_3 (20–40 Ci mmol^{-1}) was obtained from American Radiolabelled Chemicals Inc, Saint Louis, MI, U.S.A. Monoclonal *anti*-haemagglutinin (HA) HA.11 (MMS-101R), clone 16B12, was obtained from BABCO, Richmond, CA, U.S.A. Chemiluminescence Western blotting kit, rat monoclonal *anti*-HA 3F10 peroxidase-conjugated IgG, was obtained from Roche Molecular Biochemicals, Indianapolis, IN, U.S.A. Polyvinylidene difluoride membrane was obtained from Amersham, Buckinghamshire, U.K. AH6809 was obtained from Tocris, U.K. $G\alpha_q$ (C19) specific antibody was obtained from Santa Cruz Laboratories, Santa Cruz, CA, U.S.A. *N*-[2-((*p*-bromocinnamyl)amino)ethyl]-5-isoquinolinesulfonamide, 2HCL (H-89) and 2-[1-(3-dimethylaminopropyl)-1H-indol-3-yl]-3-(1H-indol-3-yl)-maleimide (GF 109203X) were obtained from Calbiochem, Darmstadt, Germany. Quick Change Mutagenesis Kit was obtained from Stratagene, La Jolla, CA, U.S.A. RNasin, deoxyribonucleotides, moloney murine leukaemia virus (MMLV) Reverse Transcriptase (RT) and *Taq* DNA polymerase were obtained from Promega, Madison, WI, U.S.A. All oligonucleotides were synthesized by Sigma Genosys, Saint Louis, MO, U.S.A. Primary human mesangial cells (1° hMCs) were purchased from BioWhittaker Inc, East Rutherford, NJ, U.S.A.

MCDB131 medium was obtained from Gibco, Invitrogen Incorporation, Carlsbad, CA, U.S.A.

Methods

Subcloning and site-directed mutagenesis of TPα and TPβ

The plasmids pCMV:TPα, pBluescriptIIKS:TPβ, pcDNA3:TPα, pcDNA3:TPβ, pcDNA3:TP$^{\Delta 328}$ and pcDNA3:TPα^{S329A} have been described previously (Kinsella *et al*., 1997; Walsh *et al*., 1998; Walsh *et al*., 2000). To facilitate amino-terminal epitope tagging of proteins with the HA epitope tag (Field *et al*., 1988), the cDNAs encoding TPα, TPβ, TP$^{\Delta 328}$ and TPα^{S329A} were subcloned in-frame into the *Hind*III–*Eco*RI sites of pHM6 (Roche Molecular Biochemicals) to generate the plasmids pHM : TPα, pHM : TPβ, pHM : TP$^{\Delta 328}$ and pHM : TPα^{S329A}, respectively.

Deletion of the amino acids carboxyl to Leu^{336} of TPα was achieved by conversion of Thr^{337} codon to a Stop codon (Thr^{337}, ACG to Stop^{337}, TAA). Site-directed mutagenesis was performed by PCR mutagenesis using pCMV:TPα as template and oligonucleotides 5′-GAGAAGCTTG ATG TGG CCC AAC GGC AGT TCC-3′ (sense primer; nucleotides +1 to +21 of TPα sequence are underlined) and 5′-CT CTA AGC ***TTA*** GAC CTG GGG CTG GAG GGA-3′ (antisense primer; sequences complimentary to nucleotides +993 to +1008 of TPα sequence are underlined, and the mutator in-frame stop codon is in boldface italics). PCR amplifications were performed using Expand High Fidelity® *Taq* DNA polymerase, and the resulting PCR-amplified cDNA was subcloned into the *Hind*III–*Eco*RI site of pHM6 to generate pHM : TPα$^{\Delta 336}$.

Conversion of Thr^{337} to Ala^{337} of TPα was performed by PCR mutagenesis using pCMV : TPα as template and oligonucleotides 5′-GAGAAGCTTG ATG TGG CCC AAC GGC AGT TCC-3′ (sense primer; nucleotides +1 to +21 of TPα sequence are underlined) and 5′-TCTC GAA TT CTA CTG CAG CCC GGA GCG CTG ***CG***C GAG CTG GGG CTG GAG-3′ (antisense primer; sequences complimentary to nucleotides +996 to +1029 of TPα sequence are underlined, and the sequence complementary to mutator Thr (ACG) to Ala (GCG) codon is in boldface italics). PCR amplifications were performed using Expand High Fidelity® *Taq* DNA polymerase, and the resulting PCR-amplified cDNA was subcloned into the *Hind*III–*Eco*RI site of pHM6 to generate pHM : TPα^{T337A}.

Conversion of Ser^{331} to Ala^{331} of TPα, herein designated TPα^{S331A}, was performed using the Stratagene Quick Change site-directed mutagenesis kit using pHM : TPα as template and oligonucleotides 5′-G CCC AGG TCG CTG ***GCC*** CTC CAG CCC C-3′ (sense primer where the sequence corresponding to mutator Ser (TCC) to Ala (GCC) is in boldface italics) and 5′-G GGG CTG GAG ***GGC*** CAG CGA CCT GGG C-3′ (antisense primer; the sequence complimentary to mutator Ser (TCC) to Ala (GCC) codon is in boldface italics), resulting in the generation of the plasmid pHM : TPα^{S331A}.

Deletion of the amino acids carboxyl to Ile^{367}of TPβ was achieved by conversion of Thr^{368} codon to a Stop codon (Thr^{368}, ACA to Stop^{368}, TGA). Site-directed mutagenesis was performed by PCR mutagenesis using pBluescriptIIKS:TPβ as template and oligonucleotides 5′-GAGAAGCTTG ATG TGG CCC AAC GGC AGT TCC-3′ (sense primer; nucleotides +1 to +21 of TPβ sequence are underlined) and 5′-TCTC GAAT ***TCA*** AAT CCC AGC AGC TCG GGA-3′ (antisense primer; sequences complimentary to nucleotides +1086 to +1101 of TPβ sequence are underlined, and the mutator in-frame stop codon is in boldface italics). PCR amplifications were performed using Expand High Fidelity® *Taq* DNA polymerase, and the resulting PCR-amplified cDNA was subcloned into the *Hind*III–*Eco*RI site of pHM6 to generate pHM : TPβ$^{\Delta 367}$.

Conversion of Thr^{399} to Ala^{399} of TPβ was performed by PCR mutagenesis using pBluescriptIIKS:TPβ as template and oligonucleotides 5′-GAGAAGCTTG ATG TGG CCC AAC GGC AGT TCC-3′ (sense primer; nucleotides +1 to +21 of TPβ sequence are underlined) and 5′-TCTC GAAT TCA ATC CTT TCT GGA CAG AGC CTT CCC ***TGC*** TGG AGG TTC AAA AGG-3′ (antisense primer; sequences complimentary to nucleotides +1182 to +1221 of TPβ sequence are underlined, and the sequence complementary to mutator Thr (ACA) to Ala (GCA) codon is in boldface italics). PCR amplifications were performed using Expand High Fidelity® *Taq* DNA polymerase, and the resulting PCR-amplified cDNA was subcloned into the *Hind*III–*Eco*RI site of pHM6 to generate pHM : TPβ^{T399A}.

Conversion of Ser^{404} to Ala^{404} of TPβ was performed by PCR mutagenesis using pBluescriptIIKS : TPβ as template and oligonucleotides 5′-GAGAAGCTTG ATG TGG CCC AAC GGC AGT TCC-3′ (sense primer; nucleotides +1 to +21 of TPβ sequence are underlined) and 5′-TCTC GAAT TCA ATC CTT TCT ***GGC*** CAG AGC CTT CCC TGT-3′ (antisense primer; sequences complimentary to nucleotides +1197 to +1221 of TPβ sequence are underlined, and the sequence complementary to mutator Ser (TCC) to Ala (GCC) codon is in boldface italics). PCR amplifications were performed using Expand High Fidelity® *Taq* DNA polymerase, and the resulting PCR-amplified cDNA was subcloned into the *Hind*III–*Eco*RI site of pHM6 to generate pHM : TPβ^{S404A}.

Conversion of Thr^{399} and Ser^{404} to Ala^{399} and Ala^{404} of TPβ was performed by PCR mutagenesis using pHM : TPβ^{T399A} as template and oligonucleotides 5′-GAGAAGCTTG ATG TGG CCC AAC GGC AGT TCC-3′ (sense primer; nucleotides +1 to +21 of TPβ sequence are underlined) and 5′-TCTC GAAT TCA ATC CTT TCT ***GGC*** CAG AGC CTT CCC TGC-3′ (antisense primer; sequences complimentary to nucleotides +1197 to +1221 of TPβ sequence are underlined, and the sequence complementary to mutator Ser (TCC) to Ala (GCC) codon is in boldface italics). PCR amplifications were performed using Expand High Fidelity® *Taq* DNA polymerase, and the resulting PCR-amplified cDNA was subcloned into the *Hind*III–*Eco*RI site of pHM6 to generate pHM : TPβ^{T399A,S404A}. All plasmids and their corresponding mutations were verified by double-stranded DNA sequence analysis (MWG Biotech Ltd). The plasmid pCMV:Gα_q has previously been described (Kinsella *et al*., 1997; Hayes *et al*., 1999).

Cell culture and transfections

Primary human mesangial cells (1° hMCs) were obtained from BioWhittaker Inc. and were routinely cultured in MCDB131 medium supplemented with 10% foetal bovine serum (FBS) and maintained at 37°C in 5% CO_2. HEK 293 cells were

obtained from the American Type Culture Collection (Manassas, VA, U.S.A.) and were cultured in minimal essential medium with Earle's salts (MEM) supplemented with 10% FBS and maintained at 37°C in 5% CO_2. HEK.TPα and HEK.TPβ cell lines stably overexpressing TPα and TPβ, respectively, were previously described (Walsh M.T. *et al*., 2000). Routinely, HEK 293 cells were plated in 10 cm culture dishes at a density of 2×10^6 cells per dish in 8 ml media approximately 48 h prior to transformation, and thereafter were transiently transfected with 10 μg pADVA (Gorman *et al*., 1990) and 25 μg of pcDNA-, pCMV- or pHM-based vectors using the calcium phosphate/DNA co-precipitation procedure essentially as previously described (Kinsella *et al*., 1997). For transient transfections, cells were harvested at 48 h post transfection. To create the HEK.TPα, HEK.TPβ, HEK.TP$^{\Delta 328}$, HEK.TPα^{S329A}, HEK.TPα^{S331A}, HEK.TPα^{T337A}, HEK.TPβ$^{\Delta 367}$, HEK.TPβ^{T399A}, HEK.TPβ^{S404A}, HEK.TPβ^{T399A,S404A} cell lines stably overexpressing the HA-epitope tagged forms of TPα, TPβ or their respective variants, HEK 293 cells were transfected with 10 μg of *Sca1*-linearized pADVA plus 25 μg of the appropriate *Pvu*1-linearized pHM : TPα, pHM : TPβ, pHM : TP$^{\Delta 328}$, pHM : TPα^{S329A}, pHM : TPα^{S331A}, pHM : TPα^{T337A}, pHM : TPβ$^{\Delta 367}$, pHM : TPβ^{T399A}, pHM : TPβ^{S404A}, pHM : TPβ^{T399A,S404A} plasmids, respectively. At 48 h post-transfection, G418 (0.8 mg ml^{-1}) selection was applied and after approximately 21 days individual G418-resistant colonies were selected and individual pure clonal stable cell lines/isolates were examined for TP expression by evaluation of their radioligand-binding properties.

Radioligand-binding studies

Cells were harvested by centrifugation at $500 \times g$ at 4°C for 5 min and washed three times with ice-cold Ca^{2+}/Mg^{2+}-free phosphate-buffered saline (PBS). TP radioligand-binding assays were carried out at 30°C for 30 min in 100 μl reactions in the presence of 0–40 nM [^{3}H]SQ29,548 for Scatchard analysis or in the presence of 20 nM [^{3}H]SQ29,548 for saturation radioligand-binding experiments as previously described (Kinsella *et al*., 1997). Protein determinations were carried out using the Bradford (1976) assay.

Measurement of intracellular calcium ($[Ca^{2+}]_i$) mobilization

Measurements of intracellular calcium mobilization ($[Ca^{2+}]_i$) were made by monitoring the intensity of fluorescence from FURA2/AM preloaded cells as previously described (Kinsella *et al*., 1997). Briefly, HEK 293 stably overexpressing the various TP receptors were transiently transfected with pCMV : $G\alpha_q$ approximately 48 h prior to harvesting. Thereafter, either 1° hMCs cells or HEK 293 cell lines were harvested by scraping, were then washed twice in ice-cold PBS and then resuspended in HBSSHB (modified Ca^{2+}/Mg^{2+}-free Hank's buffered salt solution, containing 10 μM HEPES, pH 7.67, 0.1% bovine serum albumin (BSA)) buffer at 10^7 cells ml^{-1} and incubated in the dark with 5 μM FURA2/AM for 45 min at 37°C. Cells were collected by centrifugation ($900 \times g$, 5 min), washed once in an equal volume of HBSSHB, and were finally resuspended in HBSSHB buffer at 10^7 cells ml^{-1} and kept at room temperature in the dark until use. For each measurement of $[Ca^{2+}]_i$ mobilization, aliquots of cells were diluted to 0.825×10^6 cells ml^{-1} in HBSSHB buffer containing 1 mM $CaCl_2$ and FURA2 fluorescence was recorded (2 ml aliquots of cells) at 37°C with gentle stirring with a Perkin-Elmer-Cetus LS50-B spectrofluorometer at excitation wavelengths of 340 and 380 nm and an emission wavelength of 510 nm, respectively.

Cells were stimulated with the TP agonist U46619 (1 μM) at 50 s, or with 17 phenyl trinor PGE_2 (1 μM), $PGF_{2\alpha}$ (1 μM), or Misoprostol (0.7 μM) at 50 s, followed by stimulation with U46619 (1 μM) at 150 s. Alternatively, cells were pre-incubated in the presence of various kinase inhibitors {*N*-[2-((*p*-bromocinnamyl)amini)ethyl}-5-isoquinolinesulphonamide, 2HCL} (H-89, 10 μM), 2-[1-(3-dimethylaminopropyl)-1H-indol-3-yl]-3-(1H-indol-3-yl)-maleimide] (GF 109203X, 50 nM), or the EP_1 antagonist SC-19220 (0.6 μM) for 5 min prior to stimulation with the above ligands. In all cases, the drugs (agonists, antagonists and kinase inhibitors in ethanol or DMSO) were diluted in vehicle HBSSHB, at the appropriate concentration such that addition of 20 μl of the diluted drug/inhibitor to 2 ml of cells resulted in the correct working concentration. The vehicle had no effect on $[Ca^{2+}]_i$ mobilization by either TP isoforms and had no effect on experimental data. A rapid, transient rise and fall in intracellular $[Ca^{2+}]_i$ levels in response to ligand stimulation was interpreted as receptor-mediated $[Ca^{2+}]_i$ mobilization. The calibration of the signal was performed in each sample by adding 0.2% Triton X-100 to obtain the maximal fluorescence ratio (R_{max}), and then 1 mM EGTA to obtain the minimal fluorescence ratio (R_{min}). The ratio of the fluorescence at 340 nm to that at 380 nm is a measure of $[Ca^{2+}]_i$ (Grynkiewicz *et al*., 1985), which assumes a K_d of 225 nM Ca^{2+} for FURA2/AM. The results presented in the figures are representative profiles from at least four independent experiments, and are plotted as changes $[Ca^{2+}]_i$ mobilized ($\Delta[Ca^{2+}]_i$ (nM)) as a function of time (s) upon ligand stimulation. Changes in $[Ca^{2+}]_i$ mobilization were determined by measuring the peak rises in intracellular $[Ca^{2+}]_i$ mobilized ($\Delta[Ca^{2+}]_i$), and were calculated as mean changes in $\Delta[Ca^{2+}]_i \pm$ s.e.m. (nM), and values are reported at the end of each figure legend, where appropriate.

Measurement of IP_3 levels

Measurement of intracellular IP_3 levels in HEK 293 cells was made on the basis of competition between unlabelled IP_3 and a fixed concentration of [^{3}H]IP_3 for binding to an IP_3-binding protein derived from bovine adrenal glands, as described previously (Godfrey, 1992; Walsh *et al*., 2000). Routinely, cells were harvested by scraping, washed twice in ice-cold PBS and were then resuspended at approximately 2×10^6 cells/200 μl in HEPES-buffered saline (HBS; 140 nM NaCl, 4.7 mM KCl, 2.2 mM $CaCl_2$, 1.2 mM KH_2PO_4, 11 mM glucose, 15 mM HEPES-NaOH, pH 7.4) supplemented with 10 mM LiCl. Cells (200 μl) were pre-incubated at 37°C for 10 min; where appropriate, kinase inhibitors (H-89, 10 mM; GF 109203X, 50 nM) or vehicle (HBS) were added after 5 min and cells were further incubated for 5 min at 37°C. Thereafter, cells were stimulated with either U46619 (1 μM), 17 phenyl trinor PGE_2 (1 μM), or $PGF_{2\alpha}$ (1 μM) for 1 min at 37°C. Alternatively, cells were stimulated with either 17 phenyl trinor PGE_2 (1 μM) or $PGF_{2\alpha}$ (1 μM) for 1 min, followed by centrifugation at 3500 r.p.m. for 3 min, removal of buffer plus ligand and resuspension in 200 μl HBS prior to re-stimulation with

U46619 (1 μM) for 1 min at 37°C. All ligands and kinases were pre-diluted in HBS to a concentration such that 50 μl added to 200 μl of cell suspension in HBS would give the desired final concentration. To determine the basal IP_3 levels, an equivalent volume (50 μl) of the vehicle HBS was added instead of ligand. The level of IP_3 produced was quantified by radio competition assay, essentially as previously described (Godfrey, 1992). Levels of IP_3 produced by ligand-stimulated cells over basal stimulation, in the presence of HBS, were expressed in pmol $IP_3\,mg^{-1}$ protein ± s.e.m. and as fold stimulation over basal (fold increase ± s.e.m.). In all cases, four independent experiments were performed, each in duplicate.

Measurement of agonist-mediated TP phosphorylation

Whole-cell phosphorylation assays were performed essentially as previously described (Walsh *et al*., 2000). Briefly, cells (2×10^6 cells $10\,cm^{-1}$ dish) were transiently transfected with pCMV : $G\alpha_q$. Approximately, at 48 h after transfection, cells were washed once in phosphate-free Dulbecco's modified Eagle's medium (DMEM), 10% dialysed FBS, and were metabolically labelled for 60 min in the same medium ($2\,ml\,10\,cm^{-1}$ dish) containing $100\,\mu Ci\,ml^{-1}$ [^{32}P]orthophosphate ($8000–9000\,Ci\,mmol^{-1}$) at 37°C, 5% CO_2. Where appropriate, the kinase inhibitor GF 109203X (50 nM) or an equivalent volume of the vehicle (phosphate-free DMEM, 10% dialysed FBS) were added during the labelling period. Thereafter, specific ligand (20 μl) or an equivalent volume of the vehicle (phosphate-free DMEM, 10% dialysed FBS) were added to 2 ml labelling media on cells to give the final desired concentration of ligand (17 phenyl trinor PGE_2, 1 μM; or $PGF_{2\alpha}$, 1 μM) and cells were incubated at 37°C, 5% CO_2 for 10 min. Reactions were terminated by transferring the dishes to ice and aspirating the labelling medium. Cells were then washed twice in ice-cold PBS (3 ml per dish) and lysed with 0.6 ml radioimmune precipitation (RIP) buffer (50 mM Tris-Cl, pH 8.0, 150 mM NaCl, 1 mM EDTA, 1% Nonidet P-40 ($v\,v^{-1}$), 0.5% deoxycholate ($w\,v^{-1}$), 0.1% SDS ($w\,v^{-1}$), 0.5% sodium fluoride, 25 mM sodium pyrophosphate, $1\,\mu g\,ml^{-1}$ leupeptin, 0.5 mM phenyl-methylsulphonyl fluoride (PMSF), $10\,\mu g\,ml^{-1}$ aprotinin, $10\,\mu g\,ml^{-1}$ antipain and 1 mM sodium orthovanadate). Following 15 min incubation on ice, cells were harvested by scraping and disrupted by sequentially passing through hypodermic needles of decreasing bore size (G20, G21, G23 and G26), and soluble cell lysates were harvested by centrifugation for 15 min at $13{,}000 \times g$ at RT. HA-epitope-tagged TP receptors were then immunoprecipitated using the *anti*-HA 101R antibody (1 : 300 dilution) at RT for 2 h followed by the addition of 10 μl of protein G-Sepharose 4B (Sigma) and further incubation at R.T for 1 h. Immune complexes were collected by centrifugation at $13{,}000 \times g$ at R.T for 5 min and were washed three times in 0.5 ml of RIP buffer and finally resuspended in 1 × immunoprecipitation (IP) buffer (10% β-mercaptoethanol ($v\,v^{-1}$), 2% SDS ($w\,v^{-1}$), 30% glycerol ($v\,v^{-1}$), 0.025% bromophenol blue ($w\,v^{-1}$), 50 mM Tris-HCl, pH 6.8; 40 μl). Samples were loaded without boiling onto 10% polyacrylamide gels, analysed by SDS–polyacrylamide gel electrophoresis (PAGE), and thereafter electroblotted onto polyvinylidene difluoride (PVDF) membranes, essentially as described previously (Hayes *et al*., 1999). Electroblots were then exposed to Eastman Kodak Co. Xomat XAR film to detect ^{32}P-labelled proteins. Thereafter, blots were subject to phosphorimage analysis, and the intensities of phosphorylation relative to basal phosphorylation were determined and then expressed in arbitrary units of intensity relative to basal levels. In parallel experiments, cells were incubated under identical conditions in the absence of [^{32}P]orthophosphate; HA-tagged TP receptors were immunoprecipitated from the same cell lines using the *anti*-HA 101R antibody (1 : 300 dilution) and immunoblots were screened using the *anti*-HA 3F10 horseradish peroxidase conjugate antibody (1 : 600 dilution); immunoreactive proteins were visualized using the chemiluminescence sytem, as described by the manufacturer (Roche).

Reverse transcriptase–polymerase chain reaction (RT–PCR)

Total RNA was isolated from monolayer HEK 293 cells using Tri Reagent™ (Sigma), essentially as described by the supplier. Conversion of total RNA to first strand (1°) cDNA involved moloney murine leukaemia virus (MMLV) RT. Briefly, total RNA (1.4 μg) was denatured for 10 min at 70°C in the presence of random hexamer oligonucleotides (100 μM), then chilled on ice 10 × reaction buffer, deoxynucleotides, RNasin and MMLV RT (Promega) were then added to give a final reaction mix of 50 mM Tris-HCl, pH 8.3, 75 mM KCl, 3 mM $MgCl_2$, 10 mM DTT, 40 U RNasin, 0.8 mM deoxyribonucleotide triphosphate, 400 MMLV RT in a total volume of 25 μl. 1° cDNA synthesis was performed at 37°C for 40 min, then at 42°C for 40 min. Reactions were heat inactivated at 80°C for 10 min. In each RT experiment, the following negative control reactions were routinely carried out: (a) 1° cDNA reactions carried out in the absence of MMLV RT; (b) all RT reagents excluding template RNA. Aliquots (3.5 μl) of 1° cDNA were then used as templates in subsequent PCR reactions (25 μl) using primer pairs selective for EP_1: primer A: 5′ GACGCCGCTCCCGACG 3′ (sense primer) and primer B: 5′ AGAGGCGAAGCAGTTGGCG 3′ (antisense primer) of the human EP_1 gene (Funk *et al*., 1993) or FP: primer C: 5′ CTTGGTGTTTCATTGTTGTGC 3′ (sense primer) and primer D: 5′ CTAGGTGCTTGCTGATTTCTC 3′ (antisense primer) of the human FP gene (Abramovitz *et al*., 1994).

In each case, EP_1- and FP-selective primer pairs were designed to span across intron 2 of the respective EP_1 and FP genes to distinguish between products derived from first-strand cDNA to those that might be generated due to trace genomic DNA present in the total RNA preparations. In each PCR experiment, the following negative control reactions were routinely carried out for each primer pair: PCR reactions carried out in the absence of any template cDNA. Following amplification, products of the PCR reactions (7 μl) were analysed by routine agarose gel electrophoresis and the DNA/ethidium bromide complexes were visualized under ultraviolet light and photographed using a UVP GDS8000 gel documentation system.

Data analyses

Radioligand-binding data were analysed using GraphPad Prism V3.0. programme (GraphPad Software Inc., San Diego, CA, U.S.A.). Statistical analysis was carried out using the unpaired Student's *t*-test using the Statworks Analysis

package. *P*-values $\leqslant 0.05$ were considered to indicate a statistically significant difference.

Results

Effect of 17 phenyl trinor PGE_2 and $PGF_{2\alpha}$ on U46619-mediated $[Ca^{2+}]_i$ mobilization

In the current study, we sought to investigate the molecular basis of the differential sensitivities of TPα *versus* TPβ to EP_1 signalling and to identify those residues/sites within TPα and TPβ specifically targeted by EP_1 agonists (Walsh & Kinsella, 2000). Moreover, in view of the shared Gq/PLCβ effector signalling mechanism between the EP_1 and FP receptors, we sought to investigate whether the TP isoforms are subject to a similar FP-mediated cross-regulation/desensitization mechanism.

Thus, TP isoform signalling was investigated in HEK 293 cell lines stably overexpressing TPα (HEK.TPα cells) or TPβ (HEK.TPβ cells) and in primary human renal mesangial cells (1° hMCs) which have been confirmed to endogenously express both TPα and TPβ isoforms (data not shown). It has been reported that for efficient TPα and TPβ coupling to PLCβ activation in HEK 293 cells, it is necessary to co-transfect cells with a member of the G_q family of heterotrimeric G proteins (Kinsella *et al*., 1997; Walsh *et al*., 1998). Hence, throughout these studies, HEK 293-based cell lines were routinely co-transfected with pCMV : $G\alpha_q$, encoding $G\alpha_q$ (Kinsella *et al*., 1997). While stimulation of HEK.TPα cells and HEK.TPβ cells, transiently co-transfected with pCMV : $G\alpha_q$, with the TP agonist U46619 mediated a substantial rise in intracellular calcium ($[Ca^{2+}]_i$) mobilization (Figure 1a and d), consistent with previous reports (Walsh & Kinsella, 2000), 17 phenyl trinor PGE_2 significantly impaired signalling through both TPα (Figure 1b, $P=0.0005$) and TPβ (Figure 1e, $P=0.0076$) isoforms. Moreover, while stimulation of HEK.TPα and HEK.TPβ cells, transiently co-transfected with pCMV : $G\alpha_q$, with the FP agonist $PGF_{2\alpha}$ each mediated a moderate, though significant, rise in $[Ca^{2+}]_i$ mobilization (Figure 1c and f), it significantly impaired signalling through both TPα (Figure 1c, $P=0.0001$) and TPβ (Figure 1f, $P=0.0059$). The IC_{50}'s of $PGF_{2\alpha}$ in HEK.TPα and HEK.TPβ cells were 0.4 and 0.2 μM, respectively. While stimulation of 1° hMCs with U46619 yielded a substantial rise in $[Ca^{2+}]_i$ mobilization (Figure 1g), pre-stimulation of 1° hMCs with both 17 phenyl trinor PGE_2 (Figure 1h) and $PGF_{2\alpha}$ (Figure 1i) each mediated a moderate, though significant, rise in $[Ca^{2+}]_i$ mobilization and each significantly impaired TP signalling in response to secondary stimulation with U46619 (Figure 1h, $P=0.0004$; Figure 1i, $P=0.0003$). The presence of mRNA encoding EP_1 and FP receptors in HEK 293 cells (Figure 1k) and 1° hMCs (data not shown) was confirmed by RT–PCR.

Whereas we have previously established that the antagonist AH6809 significantly impaired 17 phenyl trinor PGE_2-mediated desensitization of both TPα and TPβ, owing to its lack of EP receptor selectivity (Narumiya *et al*., 1999), these data did not fully exclude the possibility that 17 phenyl trinor PGE_2 may be acting through other EP subtypes, such as through the $EP_2/EP_3/EP_4$ subtypes. Thus, we extended this investigation by examining the effect of the EP_1 selective antagonist SC-19220 (Inoue *et al*., 1999). Pre-stimulation of HEK.TPα cells and HEK.TPβ cells (Figure 2a and b) and 1° hMCs (data not shown) with SC-19220 inhibited 17 phenyl trinor PGE_2 induced $[Ca^{2+}]_i$ mobilization and impaired 17 phenyl trinor PGE_2 induced desensitization of TP signalling in response to secondary stimulation with U46619 (Figure 2a, $P=0.44$; Figure 2b, $P=0.13$, respectively). Moreover, the $EP_2/EP_3/EP_4$ agonist Misoprostol (Bunce *et al*., 1991; Walt, 1992; Smith *et al*., 1994; Talpain *et al*., 1995) did not yield significant increases in $[Ca^{2+}]_i$ mobilization and did not significantly affect subsequent U46619-mediated $[Ca^{2+}]_i$ mobilization by TPα (Figure 2c, $P=0.085$), TPβ (Figure 2d, $P=0.84$) or 1° hMCs (data not shown).

Effect of H-89 and GF 109203X on 17 phenyl trinor PGE_2- and $PGF_{2\alpha}$-mediated desensitization of TPα and TPβ signalling

To investigate whether the second-messenger PKs may be involved in 17 phenyl trinor PGE_2 and/or $PGF_{2\alpha}$ mediated cross-desensitization of TP signalling in 1° hMCs, and in the respective HEK 293 cell lines, the effect of H-89, a PKA inhibitor, and GF 109203X, a PKC inhibitor, on U46619-mediated $[Ca^{2+}]_i$ mobilization was examined. Pre-incubation of 1° hMCs with H-89 had no significant effect on either 17 phenyl trinor PGE_2- (Figure 3a, $P=0.87$) or $PGF_{2\alpha}$ (Figure 3c, $P=0.0778$) -mediated desensitization of $[Ca^{2+}]_i$ mobilization in response to U46619. In contrast, GF 109203X significantly impaired 17 phenyl trinor PGE_2 (Figure 3b, $P=0.0006$) and $PGF_{2\alpha}$ (Figure 3d, $P=0.0003$) cross-desensitization of U46619-mediated $[Ca^{2+}]_i$ responses.

H-89 had no significant effect on either $PGF_{2\alpha}$ or 17 phenyl trinor PGE_2-mediated desensitization of U46619 responses in either HEK.TPα cells (Figure 4a, panel and inset, $P=0.312$ and 1.0, respectively) or HEK.TPβ cells (Figure 4c, panel and inset, $P=0.756$ and 0.561, respectively). However, GF 109203X significantly impaired both $PGF_{2\alpha}$- and 17 phenyl trinor PGE_2-mediated desensitization of the U46619 responses in both HEK.TPα cells (Figure 4b, panel and inset, $P=0.0001$ and 0.0005, respectively) and HEK.TPβ cells (Figure 4d, panel and inset, $P=0.0056$ and 0.0068, respectively). Moreover, neither $PGF_{2\alpha}$ nor 17 phenyl trinor PGE_2 had any effect on U46619-mediated $[Ca^{2+}]_i$ mobilization by $TP^{\Delta 328}$ (Figure 4e and f; Figure 4f, panel and inset, $P=0.13$ and 0.336, respectively), a variant of TP devoid of those residues unique to TPα and TPβ. Taken together, these results indicate that EP_1- and FP-mediated desensitization of TPα and TPβ, either endogenously expressed in 1° hMCs or stably overexpressed in HEK 293 cells, occurs through a H-89-insensitive, GF 109203X-sensitive mechanism and that the target sites of this desensitization are located within the unique C-tail regions of TPα and TPβ at sites distal to Arg^{328}.

Investigation of the mechanism of 17 phenyl trinor PGE_2- and $PGF_{2\alpha}$-mediated cross-desensitization of TPα signalling

Analysis of the unique C-tail sequences of both TPα and TPβ identified the presence of several Ser/Thr residues that may represent target residues for phosphorylation. Thus, a combination of bioinformatic approaches, using the Phospho-Base program for protein sequence analysis (Blom *et al*., 1998), as well as site-directed/deletion mutagenesis were employed

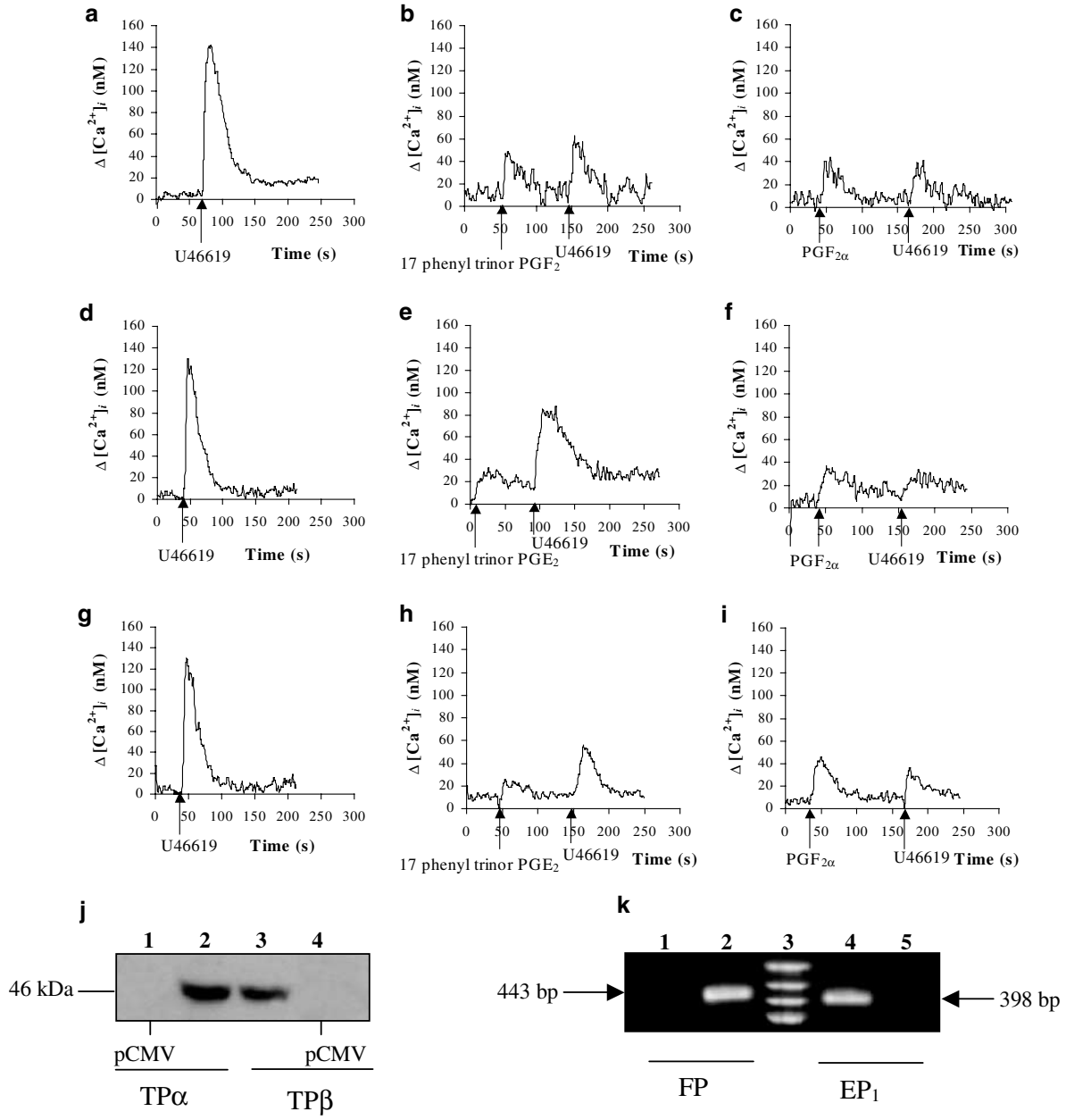

Figure 1 Effect of 17 phenyl trinor PGE_2 and $PGF_{2\alpha}$ on U46619-mediated $[Ca^{2+}]_i$ mobilization. HEK.TPα cells (panels (a–c)) or HEK.TPβ cells (panels (d–f)), transiently co-transfected with pCMV : $G\alpha_q$, and 1° hMCs (panels (g–i)) were either stimulated with 1 μM U46619 alone (panels (a, d) and (g)), or were pre-stimulated with either 1 μM 17 phenyl trinor PGE_2 (panels (b, e) and (h)) or with 1 μM $PGF_{2\alpha}$ (panels (c, f) and (i)) prior to stimulation with 1 μM U46619, where ligands were added at the times indicated by the arrows. Data presented are representative profiles from at least four independent experiments and are plotted as changes in intracellular Ca^{2+} mobilization ($\Delta[Ca^{2+}]_i$, nM) as a function of time (second, s). The actual mean changes in $[Ca^{2+}]_i$ mobilization (nM ± s.e.m.; $n = 4$) were as follows. Panel (a) U46619, $\Delta[Ca^{2+}]_i = 142 \pm 6.3$ nM; panel (b) 17 phenyl trinor PGE_2, U46619, $\Delta[Ca^{2+}]_i = 48 \pm 2.6$, 67 ± 3.4 nM; panel (c) $PGF_{2\alpha}$, U46619, $\Delta[Ca^{2+}]_i = 42 \pm 3.8$, 39 ± 3.2 nM; panel (d) U46619, $\Delta[Ca^{2+}]_i = 137 \pm 6.3$ nM; panel (e) 17 phenyl trinor PGE_2, U46619, $\Delta[Ca^{2+}]_i = 36 \pm 3.3$, 93 ± 6.2 nM; panel (f) $PGF_{2\alpha}$, U46619, $\Delta[Ca^{2+}]_i = 40 \pm 3.3$, 36 ± 17.8 nM; panel (g) U46619, $\Delta[Ca^{2+}]_i = 139 \pm 4.7$ nM; panel (h) 17 phenyl trinor PGE_2, U46619, $\Delta[Ca^{2+}]_i = 37 \pm 2.3$, 66 ± 4.7 nM; panel (i) $PGF_{2\alpha}$, U46619, $\Delta[Ca^{2+}]_i = 41 \pm 2.9$, 20 ± 8.8 nM; panel (j) HEK.TPα (lanes 1 and 2) or HEK.TPβ (lanes 3 and 4) cells transiently co-transfected with the control vector pCMV5 (lanes 1 and 4) or with pCMV : $G\alpha_q$ (lanes 2 and 3) were analysed by SDS–PAGE (75 μg whole-cell protein analysed/lane) followed by Western blot analysis using *anti*-Gαq antibody (C-19). Data presented are representative immunoblots from four independent experiments. The relative position of the 46 kDa molecular size marker is indicated to the left of panel (j). Panel (k) RT–PCR analysis of the human FP cDNA (lane 2; 443 bp) and the EP_1 cDNA (lane 4; 398 bp) amplified from total RNA isolated from HEK 293. The negative control PCRs, where amplification FP and EP_1-selective primers were added to the reaction without any template cDNA, are shown in lanes 1 and 5, respectively. Molecular size DNA markers ranging from 517 to 350 bp are shown in lane 3.

to investigate whether any of these putative phosphorylation sites within either TPα and/or TPβ represent potential target sites for either EP_1- or FP-mediated desensitization. Figure 5a and b, respectively, illustrates the C-tail sequences of TPα and TPβ and highlights the entire repertoire of site-directed or deletion mutations that were established

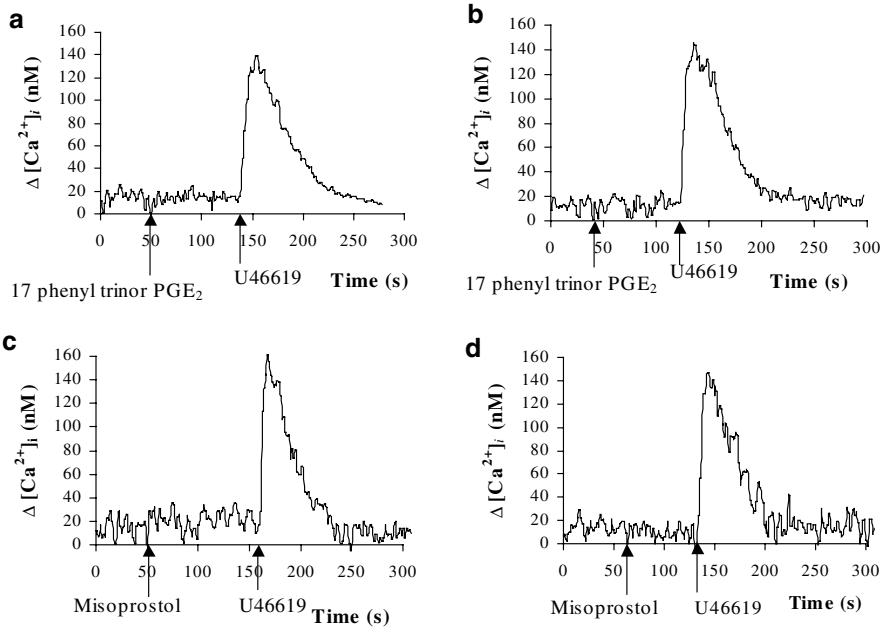

Figure 2 Effect of SC-19220 and Misoprostol on U46619-mediated $[Ca^{2+}]_i$ mobilization. HEK.TPα cells (panels (a) and (c)) and HEK.TPβ cells (panels (b) and (d)), transiently co-transfected with pCMV : $G\alpha_q$, were either pre-incubated with 0.6 μM SC-19220 for 15 min prior to stimulation with 1 μM 17 phenyl trinor PGE_2 followed by 1 μM U46619 (panels (a) and (b), respectively), or were stimulated with 0.7 μM Misoprostol (panels (c) and (d)) prior to stimulation with 1 μM U46619, where ligands were added at the times indicated by the arrows. Data presented are representative profiles from at least four independent experiments and are plotted as changes in intracellular Ca^{2+} mobilization ($\Delta[Ca^{2+}]_i$, nM) as a function of time (second, s). The actual mean changes in $[Ca^{2+}]_i$ mobilization (nM ± s.e.m.; $n=4$) were as follows: 1 μM U46619, $\Delta[Ca^{2+}]_i = 145 \pm 6.3$ nM for HEK : $TP\alpha_{10}$; 1 μM U46619, $\Delta[Ca^{2+}]_i = 139 \pm 4.7$ nM for HEK : $TP\beta_3$ (data not shown); panel (a) 17 phenyl trinor PGE_2, U46619, $\Delta[Ca^{2+}]_i = 42 \pm 2.1$, 139 ± 3.2 nM; panel (b) 17 phenyl trinor PGE_2, U46619, $\Delta[Ca^{2+}]_i = 55 \pm 3.5$, 159 ± 2.2 nM; panel (c) Misoprostol, U46619, $\Delta[Ca^{2+}]_i = 21 \pm 2.3$, 128 ± 4 nM; panel (d) Misoprostol, U46619, $\Delta[Ca^{2+}]_i = 19 \pm 2.4$ nM, 137 ± 8.1 nM.

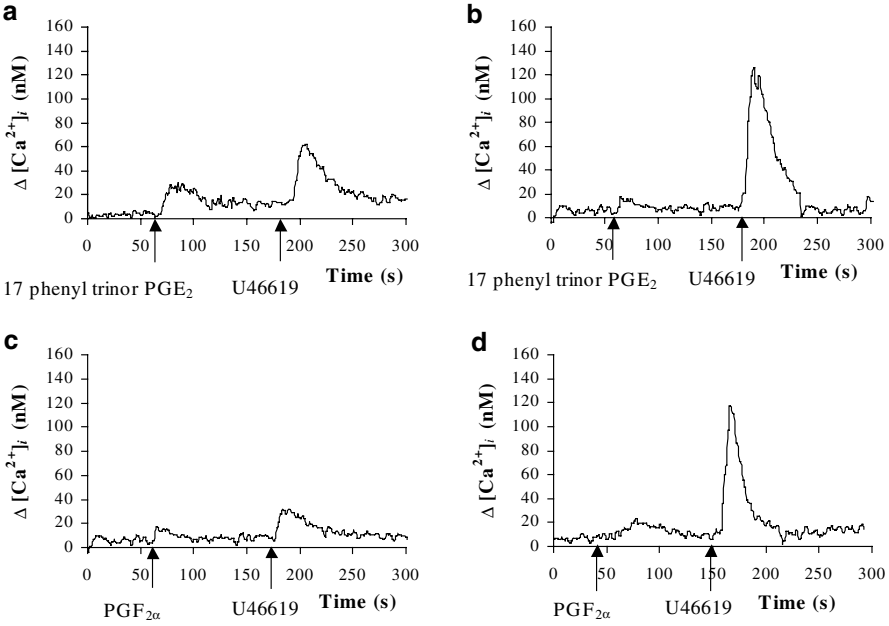

Figure 3 Effect of H-89 and GF 109203X on 17 phenyl trinor PGE_2- and $PGF_{2\alpha}$-induced inhibition of U46619-mediated $[Ca^{2+}]_i$ mobilization in 1° hMCs. 1° hMCs (panels (a–d)) were pre-incubated for 10 min with either 10 μM H-89 (panels (a) and (c)) or with 50 nM GF 109203X (panels (b) and (d)), followed by pre-stimulation with 1 μM 17 phenyl trinor PGE_2 (panels (a) and (b)) or with 1 μM $PGF_{2\alpha}$ (panels (c) and (d)) prior to stimulation with 1 μM U46619, where ligands were added at the times indicated by the arrows. Data presented are representative profiles from at least four independent experiments and are plotted as changes in intracellular Ca^{2+} mobilization ($\Delta[Ca^{2+}]_i$, nM) as a function of time (second, s). The actual mean changes in $[Ca^{2+}]_i$ mobilization (nM ± s.e.m.; $n=4$) were as follows: 1 μM U46619 alone, $\Delta[Ca^{2+}]_i = 132 \pm 3.1$ nM (data not shown). Panel (a) 17 phenyl trinor PGE_2, U46619, $\Delta[Ca^{2+}]_i = 32 \pm 2.2$, 65 ± 3.6 nM; panel (b) 17 phenyl trinor PGE_2, U46619, $\Delta[Ca^{2+}]_i = 12 \pm 1.8$, 129 ± 4.2 nM; panel (c) $PGF_{2\alpha}$, U46619, $\Delta[Ca^{2+}]_i = 17 \pm 1.3$, 42 ± 3.1 nM; panel (d) $PGF_{2\alpha}$, U46619, $\Delta[Ca^{2+}]_i = 12 \pm 1.4$, 130 ± 3.9 nM.

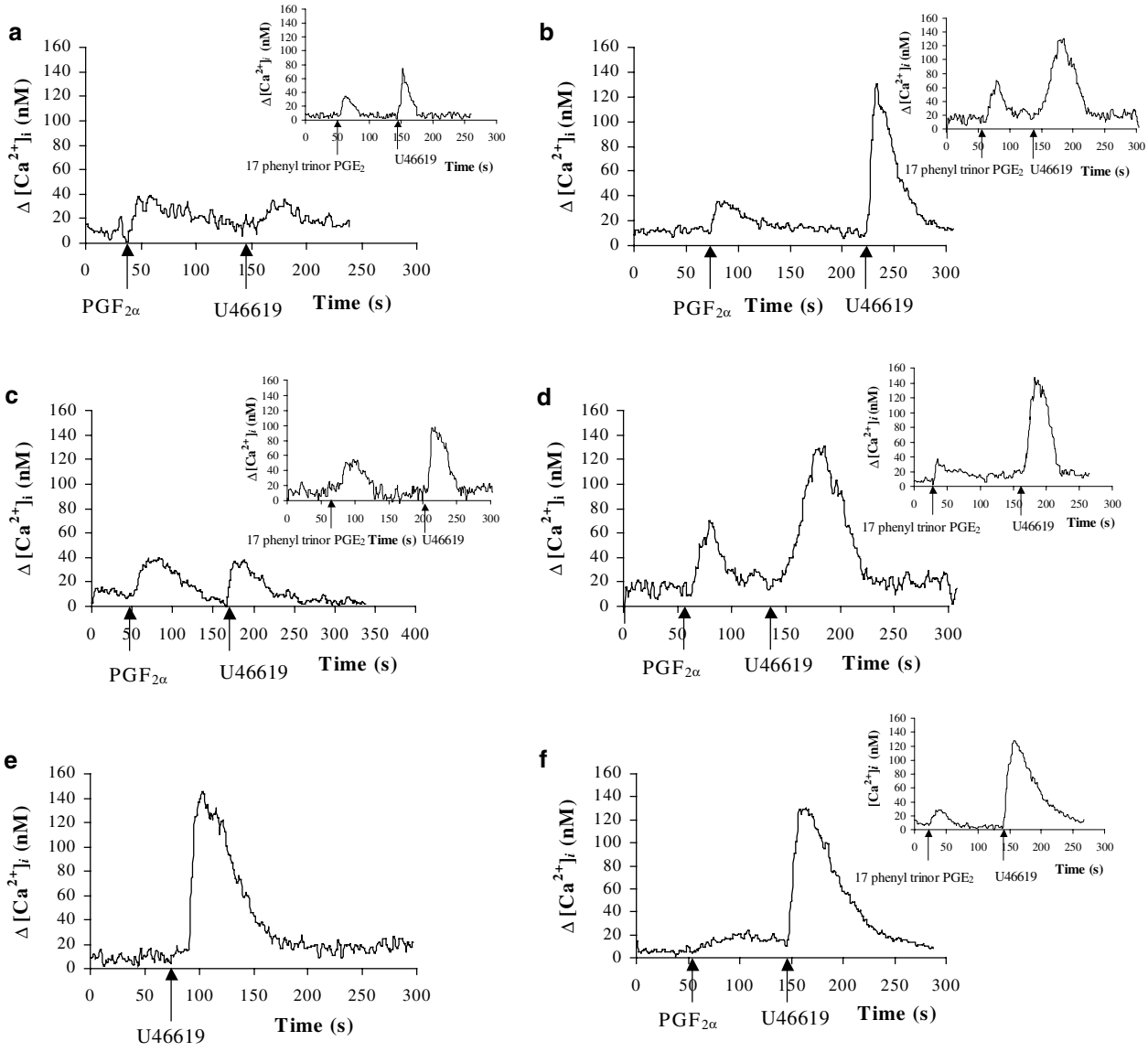

Figure 4 Effect of H-89 and GF 109203X on 17 phenyl trinor PGE_2- and $PGF_{2\alpha}$-induced inhibition of U46619-mediated $[Ca^{2+}]_i$ mobilization in HEK 293 cells. Panels/insets (a–d) HEK.TPα cells (panels/insets (a) and (b)) or HEK.TPβ cells (panels/insets (c) and (d)), transiently co-transfected with pCMV : $G\alpha_q$, were pre-incubated for 10 min with either 10 μM H-89 (panels/insets (a) and (c)) or with 50 nM GF 109203X (panels/insets (b) and (d)). Thereafter, cells were stimulated with either 1 μM 17 phenyl trinor PGE_2 prior to stimulation with 1 μM U46619 (insets (a–d)) or with 1 μM $PGF_{2\alpha}$ prior to stimulation with 1 μM U46619 (panels (a–d)), where ligands were added at the times indicated by the arrows. Panels/insets (e) and (f) HEK.$TP^{\Delta 328}$ cells, transiently co-transfected with pCMV : $G\alpha_q$, were stimulated with 1 μM U46619 alone (panel (e)), or were stimulated with 1 μM 17 phenyl trinor PGE_2 prior to stimulation with 1 μM U46619 (inset (f)) or with 1 μM $PGF_{2\alpha}$ prior to stimulation with 1 μM U46619 (panel (f)). Data presented are representative profiles from at least four independent experiments, and are plotted as changes in intracellular Ca^{2+} mobilization ($\Delta[Ca^{2+}]_i$, nM) as a function of time (second, s). Actual mean changes in $[Ca^{2+}]_i$ mobilization (nM ± s.e.m.; $n=4$) were as follows: 1 μM U46619, $\Delta[Ca^{2+}]_i = 156 \pm 5.5$ nM for HEK : TPα, and 1 μM U46619, $\Delta[Ca^{2+}]_i = 136 \pm 3$ nM for HEK : TPβ (data not shown); panel (a) $PGF_{2\alpha}$, U46619, $\Delta[Ca^{2+}]_i = 20 \pm 3.4$, 27.3 ± 9.6 nM, inset A: 17 phenyl trinor PGE_2, U46619, $\Delta[Ca^{2+}]_i = 54 \pm 4.3$, 67 ± 4.1 nM; panel (b) $PGF_{2\alpha}$, U46619, $\Delta[Ca^{2+}]_i = 36 \pm 4.2$, 139 ± 4.5 nM, inset (b) 17 phenyl trinor PGE_2, U46619, $\Delta[Ca^{2+}]_i = 49 \pm 5.3$, 135 ± 5.7 nM; panel (c) $PGF_{2\alpha}$, U46619, $\Delta[Ca^{2+}]_i = 35 \pm 3.9$, 30 ± 2.6 nM, inset (c) 17 phenyl trinor PGE_2, U46619, $\Delta[Ca^{2+}]_i = 50 \pm 4.8$, 97 ± 1.2 nM; panel (d) $PGF_{2\alpha}$, U46619, $\Delta[Ca^{2+}]_i = 60 \pm 5.8$, 136 ± 4.7 nM, inset (d) 17 phenyl trinor PGE_2, U46619, $\Delta[Ca^{2+}]_i = 34 \pm 3.2$, 140 ± 6.7 nM; panel (e) U46619, $\Delta[Ca^{2+}]_i = 146 \pm 7.9$ nM; panel (f) $PGF_{2\alpha}$, U46619, $\Delta[Ca^{2+}]_i = 12 \pm 1.8$, 129 ± 4.2 nM; inset (f) 17 phenyl trinor PGE_2, U46619, $\Delta[Ca^{2+}]_i = 42 \pm 4.3$, 133 ± 8.9 nM.

to identify their target sites for either EP_1- or FP-mediated desensitization.

In terms of TPα sequences, the following variants were initially generated: $TP\alpha^{S329A}$ in which Ser^{329} was mutated to Ala^{329}, thereby disrupting the phosphorylation site within TPα (RPRS^{329}LSL); $TP\alpha^{S331A}$ in which Ser^{331} was mutated to Ala^{331}, thereby disrupting the potential phosphorylation site (RSLS^{331}LQP) and $TP\alpha^{\Delta 336}$, a truncated variant of TPα devoid of all C-tail residues distal to Leu^{336} (Figure 5a).

Stable cell lines overexpressing HA-epitope-tagged forms of these TPα variants were established and were initially characterized by Scatchard analysis (Table 1). Neither the presence of the HA-epitope tag nor the specific mutation *per se* affected the radioligand-binding properties (K_d or B_{max}) of the

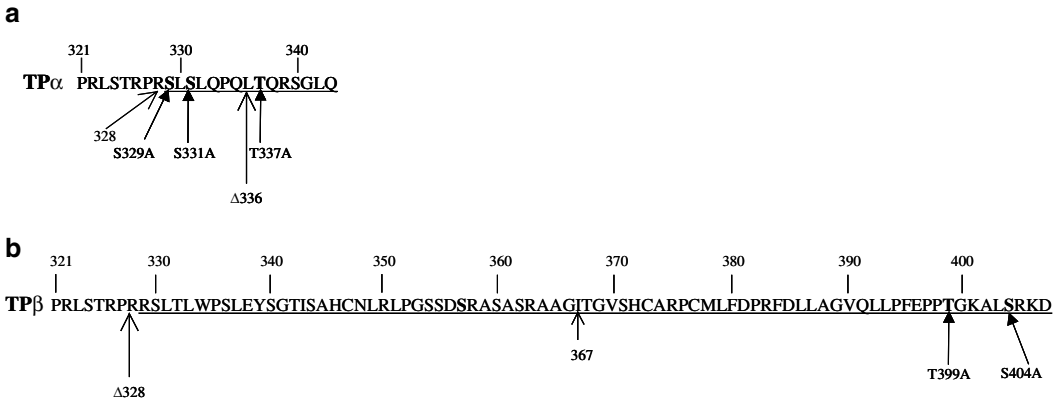

Figure 5 Amino-acid sequence of the C-tail domains of TPα and TPβ. The amino-acid sequence of the C-tail domains of TPα (residues 321–343) and of TPβ (residues 321–407) are illustrated in panels (a) and (b), respectively, where residues unique to TPα (residues 329–343) and TPβ (residues 329–407) are underlined in each case. Amino-acid residues that were mutated in TPα or TPβ to generate $TP\alpha^{S329A}$ (S329A), $TP\alpha^{S331A}$ (S331A), $TP\alpha^{T337A}$ (T337A) or $TP\beta^{T399A}$ (T399A), $TP\beta^{S404A}$ (S404A) are indicated by the solid arrows in the respective panels (a) and (b), while those residues that were converted to Stop codons to generate the truncation mutants (indicated by the Δ symbol) following amino acids $TP^{\Delta328}$ (R328), $TP\alpha^{\Delta336}$ (L336) or $TP\beta^{\Delta367}$ (I367) within TPα and/or TPβ are indicated by the open arrow heads in panels (a) and (b), respectively. An additional mutant $TP\beta^{T399A,S404A}$ was established whereby both Thr^{399}, Ser^{404} were converted to Ala^{399}, Ala^{404} in TPβ (not shown in panel (b)).

Table 1 Scatchard analysis

Cell lines	K_d (nM ± s.e.)	B_{max} (pmol mg^{-1} protein ± s.e)
HEK.TPα	10.5 ± 1.1	4.52 ± 0.05
HEK.$TP^{\Delta328}$	7.0 ± 0.9	2.33 ± 0.10
HEK.$TP\alpha^{S329A}$	9.6 ± 0.9	6.01 ± 0.16
HEK.$TP\alpha^{S331A}$	6.3 ± 1.2	4.00 ± 0.04
HEK.$TP\alpha^{\Delta336}$	7.8 ± 2.1	4.43 ± 0.04
HEK.$TP\alpha^{T337A}$	6.5 ± 1.7	4.23 ± 0.04
HEK.TPβ	9.9 ± 0.5	3.64 ± 0.02
HEK.$TP\beta^{\Delta367}$	6.7 ± 1.9	3.08 ± 0.03
HEK.$TP\beta^{T399A}$	7.3 ± 1.7	3.07 ± 0.04
HEK.$TP\beta^{S404A}$	9.4 ± 3.1	3.54 ± 0.04
HEK.$TP\beta^{T399A,S404A}$	8.3 ± 1.8	3.59 ± 0.05

For Scatchard analysis, radioligand-binding assays were carried out on HEK 293 cells stably overexpressing HA-epitope-tagged forms of wild TPα or TPβ or their respective variant receptors using the TP antagonist [^{3}H]SQ29,548 (50.4 Ci mmol^{-1}, 0–40 nM) and 75 μg whole-cell protein per assay. Radioligand-binding data were analysed using GraphPrism 3 (GraphPad Software Inc.) to determine the K_d and B_{max} values. Data presented are the mean values of four independent experiments ± standard error (s.e.). Control HEK 293 cells expressed 154 ± 4.1 fmol mg^{-1} protein ± s.e. ($n = 3$).

TPα or its variant receptors (Table 1). Moreover, stimulation of HEK.$TP\alpha^{S329A}$, HEK.$TP\alpha^{S331A}$ and HEK.$TP\alpha^{\Delta336}$ cells, each transiently co-transfected with $G\alpha_q$, with U46619 (1 μM) led to efficient $[Ca^{2+}]_i$ mobilization (Figure 6a, d and g, respectively) that was not significantly different to that of HEK.TPα cells. Pre-stimulation of both HEK.$TP\alpha^{S329A}$ or HEK.$TP\alpha^{S331A}$ cells with either 17 phenyl trinor PGE_2 (Figure 6b, $P = 0.01$; Figure 6e, $P = 0.0007$) or $PGF_{2\alpha}$ (Figure 6c, $P = 0.0001$; Figure 6f, $P = 0.0001$) each desensitized $[Ca^{2+}]_i$ mobilization in response to secondary stimulation with U46619 to levels that were not significantly different from those of the wild-type TPα ($P > 0.05$). However, in contrast, pre-stimulation of HEK.$TP\alpha^{\Delta336}$ cells with either 17 phenyl trinor PGE_2 (Figure 6h, $P = 0.85$) or $PGF_{2\alpha}$ (Figure 6i, $P = 0.86$) did not affect subsequent U46619-mediated $[Ca^{2+}]_i$ mobilization.

Further bioinformatic analysis (Blom *et al*., 1998) identified the presence of a unique consensus PKC phosphorylation site within the C-tail of TPα, with the sequence PQL$\underline{T}^{337}$QRS of TPα, where Thr^{337} represents the putative target residue for PKC phosphorylation. Thus, to investigate whether this latter consensus site may represent a target site for either 17 phenyl trinor PGE_2- or $PGF_{2\alpha}$-mediated desensitization of TPα, the critical Thr^{337} was mutated to Ala^{337} to generate the variant $TP\alpha^{T337A}$. A stable HEK 293 cell line overexpressing a HA-epitope-tagged $TP\alpha^{T337A}$ was established and was characterized by Scatchard analysis (Table 1). Stimulation of $TP\alpha^{T337A}$ cells, transiently co-transfected with $G\alpha_q$, with U46619 led to efficient $[Ca^{2+}]_i$ mobilization (Figure 6j). Moreover, pre-stimulation of HEK.$TP\alpha^{T337A}$ cells with either 17 phenyl trinor PGE_2 (Figure 6k, $P = 0.746$) or $PGF_{2\alpha}$ (Figure 6l, $P = 0.63$) did not significantly desensitize agonist-mediated $[Ca^{2+}]_i$ mobilization in response to secondary stimulation with U46619.

To further investigate the effects of EP_1 and FP activation on TPα signalling, the effect of 17 phenyl trinor PGE_2 or $PGF_{2\alpha}$ on U46619-induced IP_3 generation by TPα and $TP\alpha^{T337A}$ was evaluated. Stimulation of HEK.TPα and HEK.$TP\alpha^{T337A}$ cells with U46619 resulted in a three-fold increase in IP_3 levels (Figure 7a/b and c, respectively). Pre-incubation of HEK.TPα cells with either 17 phenyl trinor PGE_2 or $PGF_{2\alpha}$ each mediated a modest, though significant rise in IP_3 levels (Figure 7a and b, respectively), but each significantly reduced agonist-mediated IP_3 generation in response to secondary stimulation of cells with U46619 (Figure 7a, $P < 0.003$; Figure 7b, $P < 0.0001$, respectively). Moreover, GF 109203X, but not H-89, blocked both 17 phenyl trinor PGE_2- and $PGF_{2\alpha}$-mediated desensitization of TPα signalling (Figure 7a, $P < 0.01$; Figure 7b, $P < 0.0002$, respectively). In contrast, pre-incubation of HEK.$TP\alpha^{T337A}$ cells with either 17 phenyl trinor PGE_2 ($P > 0.6$) or $PGF_{2\alpha}$ ($P > 0.6$) did not significantly reduce U46619-mediated IP_3 generation by $TP\alpha^{T337A}$ (Figure 7b).

Thereafter, whole-cell phosphorylation assays were performed to establish whether TPα or $TP\alpha^{T337A}$ are direct targets for either EP_1- or FP-induced PKC phosphorylation. Initially,

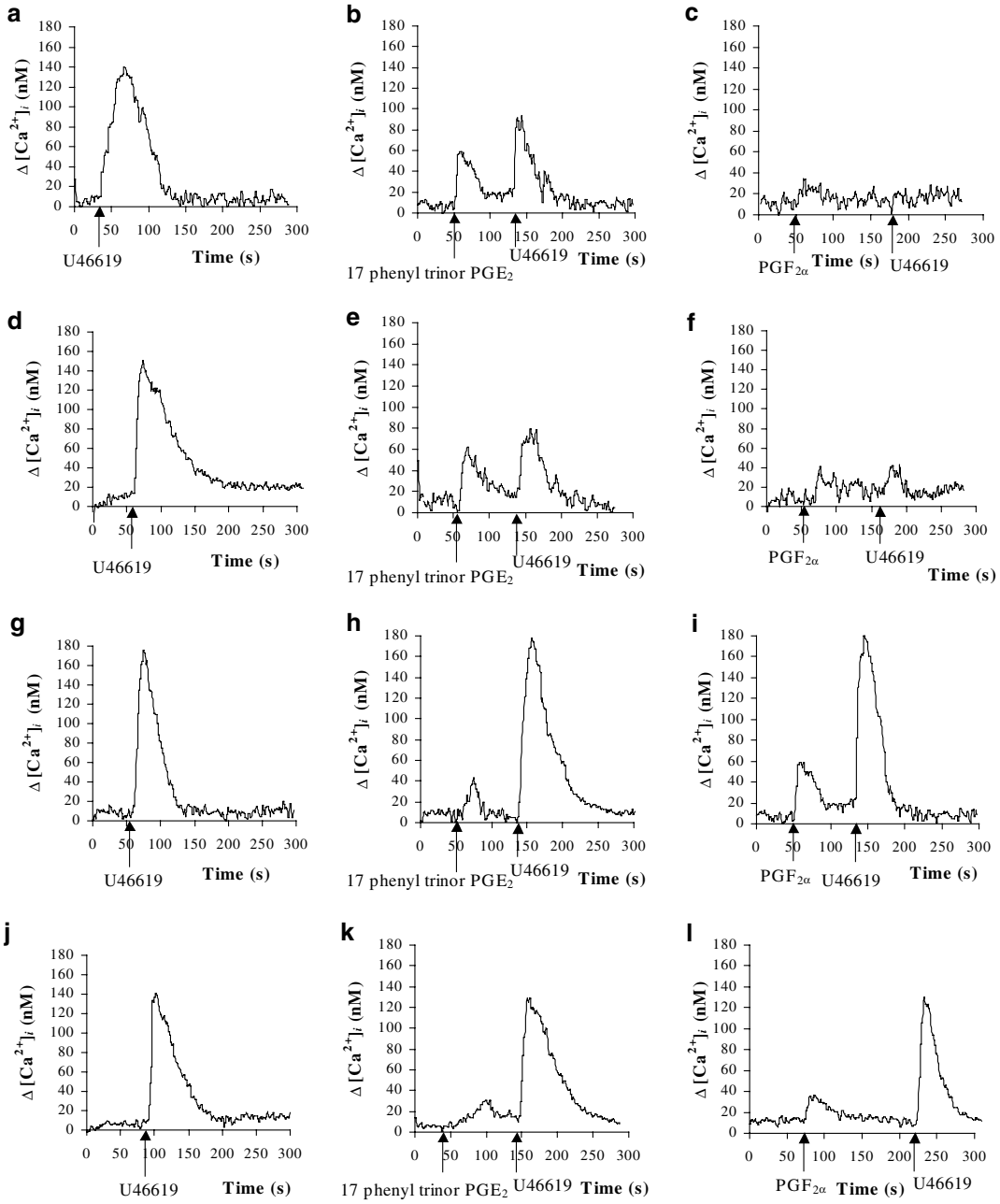

Figure 6 Effect of 17 phenyl trinor PGE_2 and $PGF_{2\alpha}$ on U46619-mediated $[Ca^{2+}]_i$ mobilization by $TP\alpha^{S329A}$, $TP\alpha^{S331A}$, $TP\alpha^{\Delta336}$ and $TP\alpha^{T337A}$. HEK.$TP\alpha^{S329A}$ cells (panels (a–c)), HEK.$TP\alpha^{S331A}$ cells (panels (d–f)), HEK.$TP\alpha^{\Delta336}$ cells (panels (g–i)) and HEK.$TP\alpha^{T337A}$ cells (panels (j–l)), transiently co-transfected with pCMV : $G\alpha_q$, were stimulated with 1 μM U46619 alone (panels (a, d, g) and (j)), or were pre-stimulated with 1 μM 17 phenyl trinor PGE_2 (panels (b, e, h) and (k)) or with 1 μM $PGF_{2\alpha}$ (panels (c, f, i) and (l)) prior to stimulation with 1 μM U46619, where ligands were added at the times indicated by the arrows. Data presented are representative profiles from at least four independent experiments and are plotted as changes in intracellular Ca^{2+} mobilization ($\Delta[Ca^{2+}]_i$, nM) as a function of time (second, s). The actual mean changes in $[Ca^{2+}]_i$ mobilization (nM $\pm$ s.e.m.; $n=4$) were as follows: panel (a) U46619, $\Delta[Ca^{2+}]_i = 139 \pm 6.5$ nM; panel (b) 17 phenyl trinor PGE_2, U46619, $\Delta[Ca^{2+}]_i = 40 \pm 9.3$, 87 ± 9.4 nM; panel (c) $PGF_{2\alpha}$, U46619, $\Delta[Ca^{2+}]_i = 39 \pm 3.6$, 26 ± 3.2 nM; panel (d) U46619, $\Delta[Ca^{2+}]_i = 156 \pm 5.7$ nM; panel (e) 17 phenyl trinor PGE_2, U46619, $\Delta[Ca^{2+}]_i = 61 \pm 2.3$, 82 ± 5.3 nM; panel (f) $PGF_{2\alpha}$, U46619, $\Delta[Ca^{2+}]_i = 31 \pm 3.4$, 22 ± 2.2 nM; panel (g) U46619, $\Delta[Ca^{2+}]_i = 177 \pm 8.2$ nM; panel (h) 17 phenyl trinor PGE_2, U46619, $\Delta[Ca^{2+}]_i = 41 \pm 3.8$, 175 ± 6.1 nM; panel (i) $PGF_{2\alpha}$, U46619, $\Delta[Ca^{2+}]_i = 57 \pm 4.5$, 179 ± 7.3 nM; panel (j) U46619, $\Delta[Ca^{2+}]_i = 130 \pm 7.5$ nM; panel (k) 17 phenyl trinor PGE_2, U46619, $\Delta[Ca^{2+}]_i = 39 \pm 3.1$, 133 ± 4.3 nM; panel (l) $PGF_{2\alpha}$, U46619, $\Delta[Ca^{2+}]_i = 23 \pm 3.5$, 135 ± 6.1 nM.

the ability of the *anti*-HA 101R antisera to immunoprecipitate the HA-epitope-tagged TPα or $TP\alpha^{T337A}$ from their respective stable cell lines, but not from the control HEK 293 cell line, was confirmed (Figure 8c). Discrete protein bands of approximately 39 kDa and broad protein bands of 46–60 kDa, representing the nonglycosylated and glycosylated forms of TPα and $TP\alpha^{T337A}$, were immunoprecipitated from HEK.TPα and HEK.$TP\alpha^{T337A}$ cells, but were not present in the immunoprecipitates from control HEK 293 cells (Figure 8c). Stimulation of HEK.TPα cells with either 17 phenyl trinor

PGE_2 or $PGF_{2\alpha}$ resulted in a significantly higher level of TPα phosphorylation relative to the level of basal phosphorylation observed in vehicle-treated cells (Figure 8a, lanes 1, 2, 4). Pre-incubation of HEK.TPα cells with GF 109203X significantly impaired TPα phosphorylation in response to subsequent stimulation with 17 phenyl trinor PGE_2 or $PGF_{2\alpha}$ (Figure 8a, lanes 3 and 5). On the other hand, stimulation of HEK.$TP\alpha^{T337A}$ cells with 17 phenyl trinor PGE_2 or $PGF_{2\alpha}$ did not increase the level of phosphorylation of $TP\alpha^{T337A}$ relative to vehicle-treated cells (Figure 8b, lanes 1, 2, 4), and pre-incubation of HEK.$TP\alpha^{T337A}$ cells with GF 109203X had no significant effect on the level of $TP\alpha^{T337A}$ phosphorylation (Figure 8c, lanes 3 and 5). Taken together, these data confirm that TPα is subject to EP_1- and FP-mediated desensitization through a GF 109203X-sensitive PKC mechanism and establish that Thr^{337}, located within the unique C-tail of TPα, represents the target site for both 17 phenyl trinor PGE_2 and $PGF_{2\alpha}$-induced phosphorylation and desensitization of signalling.

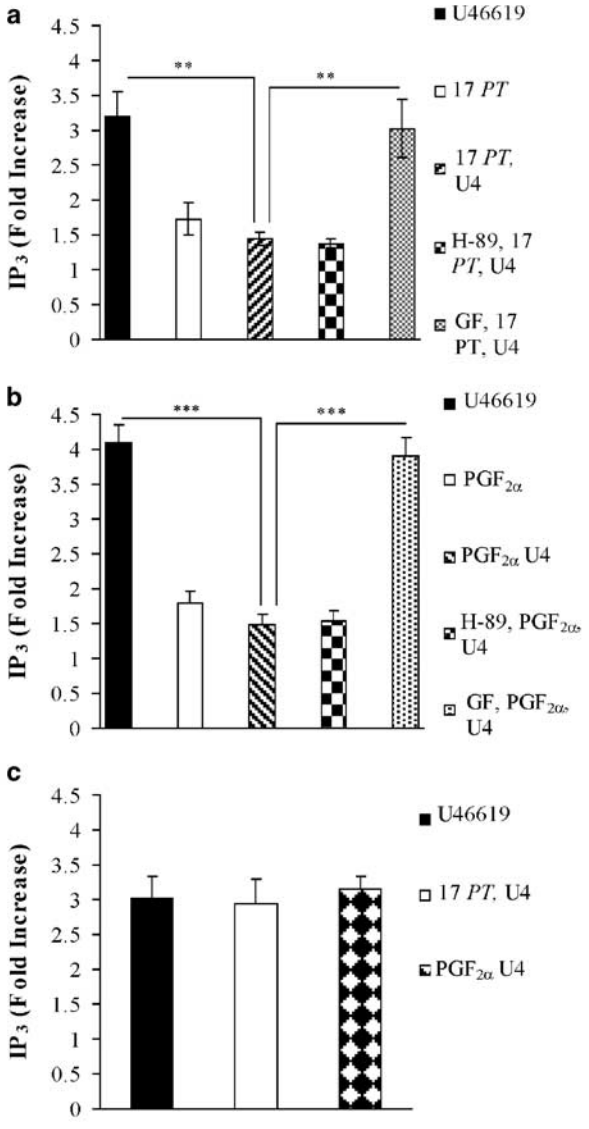

Investigation of the mechanism of 17 phenyl trinor PGE_2- and $PGF_{2\alpha}$-mediated cross-desensitization of TPβ signalling

Similarly, analysis of the amino-acid sequence of the unique C-tail domain of TPβ identified the presence of several Ser/Thr residues (15 in total) that may represent potential protein phosphorylation sites. Therefore, to localize the region within the C-tail of TPβ specifically targeted by PKC in response to EP_1/FP activation $TP\beta^{\Delta 367}$, a truncated variant of TPβ devoid of those residues distal to amino acid 367 was initially generated. Neither the presence of the HA-epitope tag nor the specific mutation *per se* affected the radioligand-binding properties (K_d or B_{max}) of TPβ or its variant receptors (Table 1). Stimulation of HEK.$TP\beta^{\Delta 367}$ cells, transiently co-transfected with $G\alpha_q$, with U46619 yielded efficient $[Ca^{2+}]_i$ mobilization (Figure 9a) to levels that were not significantly different to that of TPβ itself. Pre-stimulation of HEK.$TP\beta^{\Delta 367}$ cells with either 17 phenyl trinor PGE_2 (Figure 9b, $P=0.84$) or $PGF_{2\alpha}$ (Figure 9c, $P=0.92$) did not significantly impair $[Ca^{2+}]_i$ mobilization in response to secondary stimulation with U46619. These data indicate that the target site for both 17 phenyl trinor PGE_2 and $PGF_{2\alpha}$-mediated desensitization of TPβ signalling is located distal to Ile^{367}.

Further sequence analysis identified the presence of two putative PKC consensus phosphorylation sites within TPβ distal to Ile^{367}, with the sequence EPP$\underline{T}^{399}$GKAL$\underline{S}^{404}$RKD, where Thr^{399} and Ser^{404} represent the putative phospho-targets (Blom *et al*., 1998). Hence, site-directed mutagenesis was employed to generate the variant $TP\beta^{T399A,S404A}$, $TP\beta^{T399A}$ and $TP\beta^{S404A}$, whereby critical Thr^{399} and Ser^{404} were mutated to Ala^{399} and Ala^{404} either collectively or individually. Scatchard analyses confirmed that the mutations *per se* did not affect the ligand properties of the variant TPβ receptors (Table 1) and stimulation of HEK.$TP\beta^{T399A,S404A}$, HEK.$TP\beta^{T399A}$ and

Figure 7 Effect of 17 phenyl trinor PGE_2 and $PGF_{2\alpha}$ on U46619-mediated IP_3 generation by TPα and $TP\alpha^{T337A}$. HEK.TPα cells (panels (a) and (b)) or HEK.$TP\alpha^{T337A}$ cells (panel (c)), transiently co-transfected with pCMV : $G\alpha_q$, were stimulated at 37°C with 1 μM U46619 (U46619), 1 μM 17 phenyl trinor PGE_2 (17 *PT*), 1 μM $PGF_{2\alpha}$ ($PGF_{2\alpha}$) for 1 min or pre-stimulated with either 1 μM 17 phenyl trinor PGE_2 or 1 μM $PGF_{2\alpha}$ for 1 min, followed by 1 μM U46619 for 1 min (17 *PT*, U4; $PGF_{2\alpha}$, U4). Alternatively, cells, were pre-incubated with 10 μM H-89 for 5 min prior to pre-stimulation with either 1 μM 17 phenyl trinor PGE_2 or 1 μM $PGF_{2\alpha}$ for 1 min, followed by 1 μM U46619 for 1 min (H-89, 17 *PT*, U4; H-89, $PGF_{2\alpha}$, U4) or with 50 nM GF 109203X for 5 min prior to pre-stimulation with either 1 μM 17 phenyl trinor PGE_2 or 1 μM $PGF_{2\alpha}$ for 1 min, followed by 1 μM U46619 for 1 min (GF, 17 *PT*, U4; GF, $PGF_{2\alpha}$, U4). In each case, basal levels of IP_3 were determined by exposing cells to the vehicle HBS under identical incubation conditions. Levels of IP_3 produced in ligand-stimulated cells relative to the vehicle (HBS)-treated cells (basal IP_3) were expressed as fold stimulation of basal (fold increase in $IP_3 \pm$ s.e.m.; $n=4$). Data presented are the mean values of four independent experiments, each carried out in duplicate. The basal level of IP_3 in HEK : TPα cells was 0.42 ± 0.07 nmol mg^{-1}; HEK.$TP\alpha^{T337A}$ cells was 0.38 ± 0.05 nmol mg^{-1}. The asterisks indicate that U46619-mediated IP_3 generation was significantly reduced following pre-stimulation with 17 phenyl trinor PGE_2 and/or $PGF_{2\alpha}$ compared to cells stimulated with U46619 alone. In addition, the asterisks indicate that GF 109203X significantly blocked 17 phenyl trinor PGE_2- or $PGF_{2\alpha}$-mediated inhibition of U46619-induced IP_3 generation by TPα, where *, ** and *** indicate $P \leqslant 0.05$, $P \leqslant 0.02$ and $P \leqslant 0.001$, respectively.

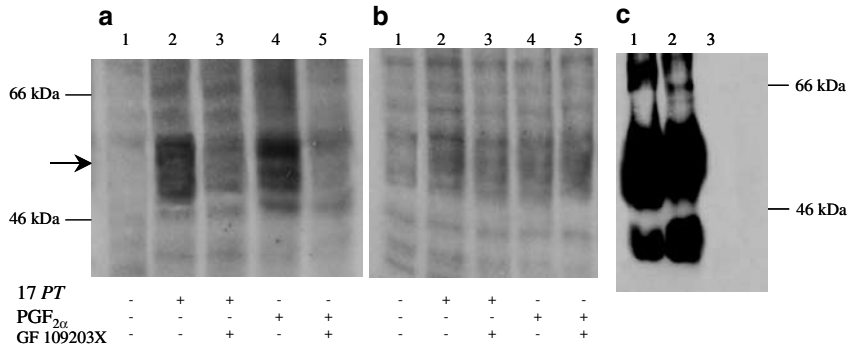

Figure 8 EP_1- and $PGF_{2\alpha}$-mediated phosphorylation of TPα and $TP\alpha^{T337A}$. HEK.TPα (panel (a)) and HEK.$TP\alpha^{T337A}$ (panel (b)) cells were labelled with [^{32}P]orthophosphate for 60 min and then stimulated for 10 min with vehicle HBS (lane 1), 1 μM 17 phenyl trinor PGE_2 (lane 2), 1 μM $PGF_{2\alpha}$ (lane 4); alternatively, cells were labelled for 60 min with [^{32}P]orthophosphate in the presence of 50 nM GF 109203X prior to stimulation for 10 min with 1 μM 17 phenyl trinor PGE_2 (lanes 3) or 1 μM $PGF_{2\alpha}$ (lanes 5). HA-tagged TPα and $TP\alpha^{T337A}$ receptors were immunoprecipitated, subjected to SDS–PAGE, electroblotted onto a PVDF membrane, followed by exposure to Xomat XAR-5 film (Kodak) for 14 days. Thereafter, blots were subject to Phosphor Image analysis and the intensities of phosphorylation relative to basal levels were determined and expressed, in arbitrary units, as follows: TPα, vehicle, 0.4-fold; 17 phenyl trinor PGE_2, 3.1-fold; GF 109203X, 17 phenyl trinor PGE_2, 1.6-fold; $PGF_{2\alpha}$, 3.4-fold; GF 109203X, $PGF_{2\alpha}$, 1.9-fold; $TP\alpha^{T337A}$, vehicle, 0.6-fold; 17 phenyl trinor PGE_2, 0.8-fold; GF 109203X, 17 phenyl trinor PGE_2, 0.7-fold; $PGF_{2\alpha}$, 1-fold; GF 109203X, $PGF_{2\alpha}$, 0.9-fold. Panel (c) HEK 293 cells overexpressing HA-epitope-tagged TPα (lane 1), HA : $TP\alpha^{T337A}$ (lane 2), or as controls, HEK 293 cells (lane 3) were immunoprecipitated with *anti*-HA 101R antibody, subjected to SDS–PAGE/Western blotting, followed by screening with the *anti*-HA 3F10 peroxidase-conjugated antibody and chemiluminescence detection. The relative positions of the molecular weight markers (kDa) are indicated to the left and right of panels (a) and (c), respectively. The arrow to the left of the panels indicates the position of the phosphorylated TPα receptor. These data are representative of three independent experiments.

HEK.$TP\beta^{S404A}$ cells with U46619 each led to efficient $[Ca^{2+}]_i$ mobilization (Figure 9d, g and j) to levels that were not significantly different from that of TPβ. Stimulation of HEK.$TP\beta^{T399A,S404A}$ cells with either 17 phenyl trinor PGE_2 (Figure 9e, $P=1$) or $PGF_{2\alpha}$ (Figure 9f, $P=0.8$) did not significantly impair $[Ca^{2+}]_i$ mobilization in response to secondary stimulation with U46619, indicating that either Thr^{399} or Ser^{404} or both represent the target site(s) for 17 phenyl trinor PGE_2- and/or $PGF_{2\alpha}$-mediated desensitization of TPβ signalling. Stimulation of HEK.$TP\beta^{T399A}$ cells with either 17 phenyl trinor PGE_2 (Figure 9h, $P=0.33$) or $PGF_{2\alpha}$ (Figure 9i, $P=0.91$) had no significant effect on U46619-mediated $[Ca^{2+}]_i$ mobilization. On the other hand, stimulation of HEK.$TP\beta^{S404A}$ cells with either 17 phenyl trinor PGE_2 or $PGF_{2\alpha}$ significantly desensitized $[Ca^{2+}]_i$ mobilization in response to secondary stimulation with U46619 (Figure 9k, $P=0.0004$; Figure 9l, $P=0.0001$). These data indicate that Thr^{399}, but not Ser^{404}, represents a target site for EP_1- and FP-mediated desensitization of TPβ signalling.

Consistent with this, while stimulation of HEK.TPβ and HEK.$TP\beta^{T399A}$ cells with U46619 resulted in approximately three-fold increases in IP_3 levels (Figure 10a–c, respectively), pre-incubation of HEK.TPβ cells with either 17 phenyl trinor PGE_2 or $PGF_{2\alpha}$ significantly reduced U46619-mediated IP_3 generation (Figure 10a, $P<0.016$; Figure 10a, $P<0.0013$). In contrast, stimulation of HEK.$TP\beta^{T399A}$ cells with either 17 phenyl trinor PGE_2 ($P=0.6$) or $PGF_{2\alpha}$ ($P=0.7$) did not significantly reduce U46619-mediated IP_3 generation by $TP\beta^{T399A}$ (Figure 10b). Moreover, pre-incubation of cells with GF 109203X, but not H-89, blocked both 17 phenyl trinor PGE_2- and $PGF_{2\alpha}$-mediated desensitization of TPβ signalling (Figure 10a, $P<0.004$; Figure 10a, $P<0.001$).

Thereafter, whole-cell phosphorylation assays were performed to establish whether TPβ or $TP\beta^{T399A}$ are direct targets for either EP_1- or FP-mediated phosporylation. Initially, the ability of the *anti*-HA 101R antisera to immunoprecipitate the HA-epitope tagged TPβ or $TP\beta^{T399A}$ cells from their respective stable cell lines was investigated (Figure 11c). Discrete protein bands of approximately 46 kDa and broad protein bands of 50–60 kDa, representing the nonglycosylated and glycosylated forms of TPβ and $TP\beta^{T399A}$, respectively, were immunoprecipitated from HEK.TPβ and HEK.$TP\beta^{T399A}$, but were not present in the immunoprecipitates from control HEK 293 cells (Figure 11c). Stimulation of HEK.TPβ cells with either 17 phenyl trinor PGE_2 or $PGF_{2\alpha}$ resulted in a significantly higher level of TPβ phosphorylation than the level of basal phosphorylation observed in vehicle-treated cells (Figure 11a, lanes 1, 2, 4). Moreover, pre-incubation of cells with GF 109203X blocked the increase in TPβ phosphorylation in response to both 17 phenyl trinor PGE_2 or $PGF_{2\alpha}$ induced (Figure 11a, lanes 3 and 5). Stimulation of HEK.$TP\beta^{T399A}$ cells with either 17 phenyl trinor PGE_2 or $PGF_{2\alpha}$ did not result in any significant increase in $TP\beta^{T399A}$ phosphorylation relative to vehicle-treated cells (Figure 11b, lanes 1, 2, 4) and pre-incubation of cells with GF 109203X had no effect on that level of $TP\beta^{T399A}$ phosphorylation (Figure 11b, lanes 3 and 5). Thus, taken together, these data confirm that TPβ is subject to EP_1- and FP-mediated desensitization through a GF 109203X-sensitive, PKC mechanism and establish that Thr^{399}, located within the unique C-tail of TPβ, represents the target site for both 17 phenyl trinor PGE_2 and $PGF_{2\alpha}$ desensitization.

Discussion

We have previously established that 17 phenyl trinor PGE_2 acting through the EP_1 subtype of the PGE_2 receptor (EP) family significantly impaired signalling through TPα and TPβ and that this counter-regulation/heterologous desensitization of TP signalling occurred through a GF 109203X-sensitive

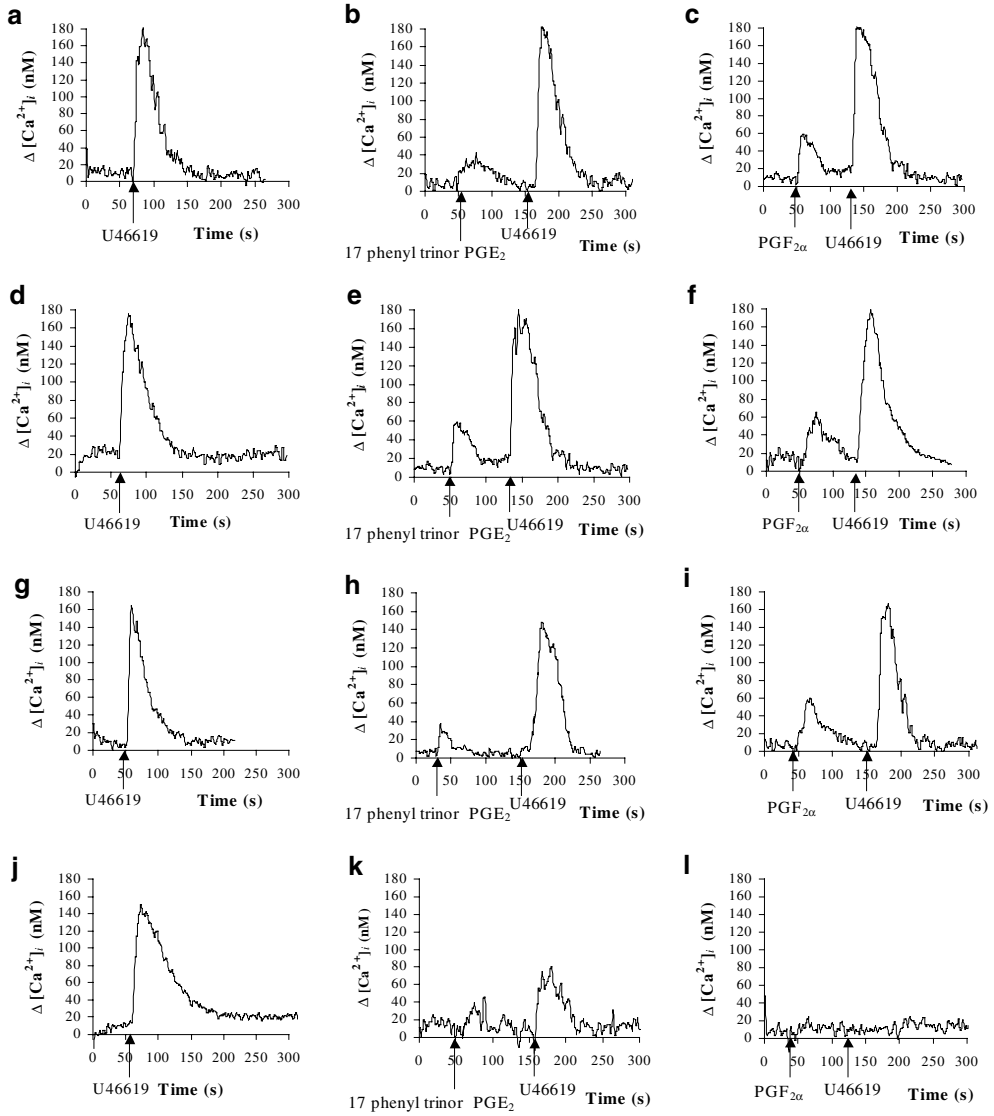

Figure 9 Effect of 17 phenyl trinor PGE_2 and $PGF_{2\alpha}$ on U46619-mediated $[Ca^{2+}]_i$ mobilization by $TP\beta^{\Delta 367}$, $TP\beta^{T399A,S404A}$, $TP\beta^{T399A}$ and $TP\beta^{S404A}$. HEK.$TP\beta^{\Delta 367}$ cells (panels (a–c)), HEK.$TP\beta^{T399A,S404A}$ cells (panels (d–f)), HEK.$TP\beta^{T399A}$ cells (panels (g–i)) and HEK.$TP\beta^{S404A}$ cells (panels (j–l)), transiently co-transfected with pCMV : $G\alpha_q$, were stimulated with 1 μM U46619 alone (panels (a, d, g) and (j)), or were pre-stimulated with 1 μM 17 phenyl trinor PGE_2 (panels (b, e, h) and (k)), or with 1 μM $PGF_{2\alpha}$ (panels (c, f, i) and (l)) prior to stimulation with 1 μM U46619, where ligands were added at the times indicated by the arrows. Data presented are representative profiles from at least four independent experiments and are plotted as changes in intracellular Ca^{2+} mobilization ($\Delta[Ca^{2+}]_i$, nM) as a function of time (second, s). Actual mean changes in $[Ca^{2+}]_i$ mobilization (nM $\pm$ s.e.m.; $n=4$) were as follows. Panel (a) U46619, $\Delta[Ca^{2+}]_i = 181 \pm 7.5$ nM; panel (b) 17 phenyl trinor PGE_2, U46619, $\Delta[Ca^{2+}]_i = 55 \pm 2.7$, 182 ± 6.2 nM; panel (c) $PGF_{2\alpha}$, U46619, $\Delta[Ca^{2+}]_i = 85 \pm 4.1$, 179 ± 5.4 nM); panel (d) U46619, $\Delta[Ca^{2+}]_i = 180 \pm 6.5$ nM; panel (e) 17 phenyl trinor PGE_2, U46619, $\Delta[Ca^{2+}]_i = 60 \pm 3.4$, 180 ± 5.2 nM; panel (f) $PGF_{2\alpha}$, U46619, $\Delta[Ca^{2+}]_i = 51 \pm 4.5$, 182 ± 4.7 nM; panel (g) U46619, $\Delta[Ca^{2+}]_i = 163 \pm 5.5$ nM; panel (h) 17 phenyl trinor PGE_2, U46619, $\Delta[Ca^{2+}]_i = 39 \pm 3.5$, 155 ± 4.7 nM; panel (i) $PGF_{2\alpha}$, U46619, $\Delta[Ca^{2+}]_i = 60 \pm 5.8$, 162 ± 6.4 nM; panel (j) U46619, $\Delta[Ca^{2+}]_i = 158 \pm 5.3$ nM; panel (k) 17 phenyl trinor PGE_2, U46619, $\Delta[Ca^{2+}]_i = 41 \pm 2.3$, 83 ± 4.3 nM; panel (l) $PGF_{2\alpha}$, U46619, $\Delta[Ca^{2+}]_i = 11 \pm 3.4$, 12 ± 2.2 nM.

mechanism, implying a possible involvement of PKC in that desensitization (Walsh & Kinsella, 2000). Moreover, the variant $TP^{\Delta 328}$ devoid of those residues unique to TPα and TPβ did not undergo EP_1-mediated desensitization, suggesting that the site(s) of EP_1-mediated desensitization may be located within the respective unique C-tail domains of TPα and TPβ (Walsh & Kinsella, 2000). In the current study, we sought to extend these studies by defining the molecular basis of the apparent differential sensitivities of TPα and TPβ to EP_1-mediated desensitization by identifying those residues/sites within TPα and TPβ specifically targeted by EP_1 signalling. Moreover, since FP receptors are abundantly co-expressed along with the TPs and EP_1 receptors in the kidney, such as in renal mesangial cells (Watabe *et al*., 1993; Abramovitz *et al*., 1994; Breyer, 1998; Sugimoto *et al*., 2000), we sought to investigate the effect of 17 phenyl trinor PGE_2 and $PGF_{2\alpha}$ on TP signalling within primary human mesangial cells (1° hMCs), comparing it to that which occurs to the individual TPα and TPβ receptors stably overexpressed in HEK 293 cells.

Stimulation of HEK.TPα, HEK.TPβ cells and 1° hMCs with the TXA_2 mimetic U46619 each yielded substantial rises in $[Ca^{2+}]_i$ mobilization. Moreover, while stimulation of the latter

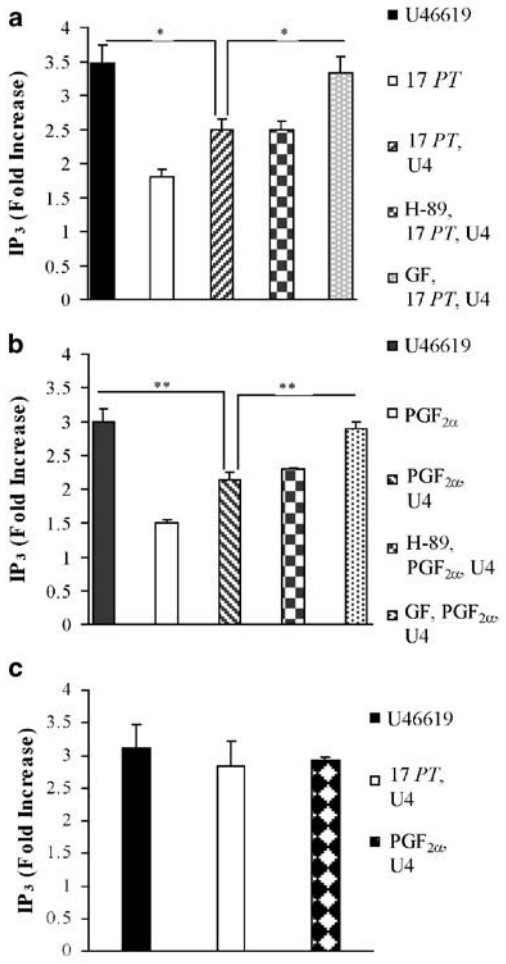

Figure 10 Effect of 17 phenyl trinor PGE_2 and $PGF_{2\alpha}$ on U46619-mediated IP_3 generation by TPβ and TPβ^{T399A}. HEK.TPβ cells (panels (a) and (b)) or HEK.TPβ^{T399A} cells (panel (c)), transiently co-transfected with pCMV : $G\alpha_q$, were stimulated at 37°C with 1 μM U46619 (U46619), 1 μM 17 phenyl trinor PGE_2 (17 *PT*), 1 μM $PGF_{2\alpha}$ ($PGF_{2\alpha}$) for 1 min, or were pre-stimulated with either 1 μM 17 phenyl trinor PGE_2 or 1 μM $PGF_{2\alpha}$ for 1 min, followed by 1 μM U46619 for 1 min (17 *PT*, U4; $PGF_{2\alpha}$, U4). Alternatively, cells were pre-incubated with 10 μM H-89 for 5 min prior to stimulation with either 1 μM 17 phenyl trinor PGE_2 or 1 μM $PGF_{2\alpha}$ for 1 min, followed by 1 μM U46619 for 1 min (H-89, 17 *PT*, U4; H-89, $PGF_{2\alpha}$, U4) or with 50 nM GF 109203X for 5 min prior to stimulation with either 1 μM 17 phenyl trinor PGE_2 or 1 μM $PGF_{2\alpha}$ for 1 min, followed by 1 μM U46619 for 1 min (GF, 17 *PT*, U4; GF, $PGF_{2\alpha}$, U4). In each case, basal levels of IP_3 were determined by exposing cells to the vehicle HBS under identical incubation conditions. Levels of IP_3 produced in ligand-stimulated cells relative to the vehicle (HBS)-treated cells (basal IP_3) were expressed as fold stimulation of basal (fold increase in $IP_3 \pm$ s.e.m.; $n = 4$). Data presented are the mean values of four independent experiments, each carried out in duplicate. The basal level of IP_3 in HEK.TPβ cells was 0.31 ± 0.06 nmol mg^{-1}, and in HEK : TPβ^{T399A} cells was 0.32 ± 0.05 nmol mg^{-1}. The asterisks indicate that U46619-mediated IP_3 generation was significantly reduced following pre-stimulation with 17 phenyl trinor PGE_2 and/or $PGF_{2\alpha}$ compared to cells stimulated with U46619 alone. In addition, the asterisks indicate that GF 109203X significantly blocked 17 phenyl trinor PGE_2- or $PGF_{2\alpha}$-mediated inhibition of U46619-induced IP_3 generation by TPβ, where *, ** and *** indicate $P \leqslant 0.05$, $P \leqslant 0.02$ and $P \leqslant 0.001$, respectively.

cell types with 17 phenyl trinor PGE_2 and $PGF_{2\alpha}$ each also yielded significant rises in $[Ca^{2+}]_i$ mobilization, confirming the expression of functional endogenous EP_1 and FP receptors in both HEK 293 cells and 1° hMCs, pre-stimulation of those cells with either ligand significantly desensitized TPα and TPβ signalling in HEK.TPα and HEK.TPβ cells, respectively, and TP signalling in 1° hMCs. The EP_1 selective antagonist SC-19220 blocked 17 phenyl trinor PGE_2-mediated desensitization of TP signalling, confirming that the latter agonist is acting through the EP_1, rather than through EP_2, EP_3, or EP_4 subtypes of the PGE_2 receptor family. Neither 17 phenyl trinor PGE_2 or $PGF_{2\alpha}$ affected signalling by $TP^{\Delta 328}$. Pre-stimulation of cells with the PKC inhibitor GF 109203X significantly impaired both EP_1- and FP-mediated desensitization of TP signalling in the respective HEK 293 cell lines and in 1° hMCs, while the PKA inhibitor H-89 had no effect on TP signalling regardless of the cell type or ligand used. Hence, these data imply that both TPα and TPβ undergo EP_1 and FP-mediated desensitization through a PKC-dependent mechanism at site(s) located within their respective unique C-tail domains.

Differences in the complement of Ser/Thr residues within the C-tail domains of TPα and TPβ indeed imply that they may be subject to independent regulation by the second messenger kinases, such as has been previously reported to occur during their differential PKA-mediated desensitization in response to PGI_2, PGD_2 and nitric oxide (Walsh *et al*., 2000; Foley *et al*., 2001; Reid & Kinsella, 2003). Hence, a combination of site-directed/deletion mutagenesis approaches was employed to identify the site(s) within the individual TPα and TPβ receptors specifically targeted EP_1- and FP-mediated desensitization. Initially, it was established that the specific mutations *per se* did not affect the ligand binding or intracellular signalling properties of the variant TPα and TPβ receptors under study. In the case of the TPα isoform, pre-stimulation of both HEK.TPα^{S329A} or HEK.TPα^{S331A} cells with either 17 phenyl trinor PGE_2 or $PGF_{2\alpha}$ each desensitized U46619-mediated $[Ca^{2+}]_i$ mobilization to levels that were not significantly different from those of the wild-type TPα. These data confirm that neither Ser^{329} nor Ser^{331} represent the site of EP_1- or FP-induced PKC desensitization, and are entirely consistent with previous reports demonstrating that Ser^{329} and Ser^{331} are specific targets for PKA (Walsh *et al*., 2000; Foley *et al*., 2001) and PKG (Wang *et al*., 1998; Yamamoto *et al*., 2001; Reid & Kinsella, 2003) phosphorylation, respectively. On the other hand, pre-stimulation of HEK.TP$\alpha^{\Delta 336}$ cells with either 17 phenyl trinor PGE_2 or $PGF_{2\alpha}$ did not affect subsequent U46619-mediated $[Ca^{2+}]_i$ mobilization, indicating that the site of PKC desensitization is located distal to Leu^{336}.

Thereafter, further bioinformatic analysis predicted the presence of a unique consensus PKC phosphorylation site (PQL$\underline{T}^{337}$QRS) within the C-tail of TPα, where Thr^{337} represents the putative phospho-target residue. Mutation of the critical Thr^{337} established that neither 17 phenyl trinor PGE_2 or $PGF_{2\alpha}$ significantly desensitized U46619-mediated $[Ca^{2+}]_i$ mobilization by TPα^{T337A}. Moreover, while both 17 phenyl trinor PGE_2 and $PGF_{2\alpha}$ each mediated modest though significant rises in IP_3 generation in both HEK.TPα and HEK.TPα^{T337A} cells, each of them reduced U46619-mediated IP_3 generation by TPα but neither ligand affected U46619-mediated IP_3 generation by TPα^{T337A}. Whole-cell phosphorylation assays established that pre-stimulation of HEK.TPα cells with either 17 phenyl trinor PGE_2 or $PGF_{2\alpha}$ significantly increased the level of TPα phosphorylation relative to vehicle-treated cells, while pre-incubation of those cells with GF

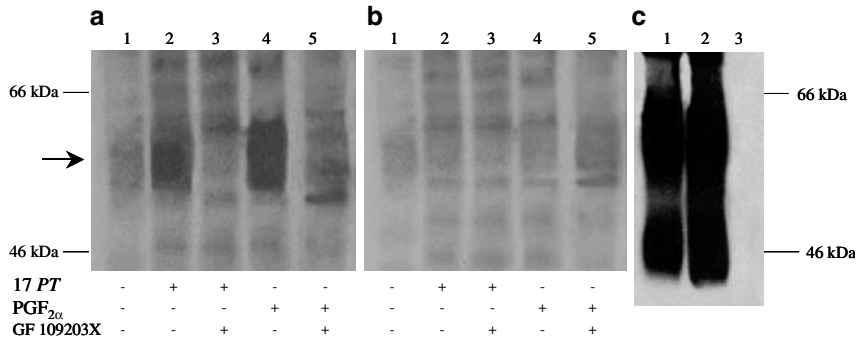

Figure 11 EP_1- and $PGF_{2\alpha}$-mediated phosphorylation of TPβ and $TP\beta^{T399A}$. HEK.TPβ (panel (a)) and HEK.$TP\beta^{T399A}$ (panel (b)) cells were labelled with [^{32}P]orthophosphate for 60 min and then stimulated for 10 min with the vehicle (lane 1), 1 μM 17 phenyl trinor PGE_2 (lane 2), 1 μM $PGF_{2\alpha}$ (lane 4); alternatively, cells were labelled for 60 min with [^{32}P]orthophosphate in the presence of 50 nM GF 109203X prior to stimulation for 10 min with 1 μM 17 phenyl trinor PGE_2 (lane 3) or 1 μM $PGF_{2\alpha}$ (lane 5). HA-tagged TPβ and $TP\beta^{T399A}$ were immunoprecipitated, subjected to SDS–PAGE, electroblotted onto PVDF membrane, followed by exposure to Xomat XAR-5 film (Kodak) for 14 days. Thereafter, blots were subject to Phosphor Image analysis and the intensities of phosphorylation relative to basal levels were determined and expressed, in arbitary units, as follows: TPβ, vehicle, 0.6-fold; 17 phenyl trinor PGE_2, 4.7-fold; GF 109203X, 17 phenyl trinor PGE_2, 1.8-fold; $PGF_{2\alpha}$, 3.1-fold; GF 109203X, $PGF_{2\alpha}$, 1.9-fold; $TP\beta^{T399A}$, vehicle, 0.5-fold; 17 phenyl trinor PGE_2, 0.7-fold; GF 109203X, 17 phenyl trinor PGE_2, 0.8-fold; $PGF_{2\alpha}$, 0.8-fold; GF 109203X, $PGF_{2\alpha}$, 0.9-fold. Panel (c) HEK 293 cells overexpressing HA-epitope-tagged TPβ (lane 1), HA : $TP\beta^{T399A}$ (lane 2), or as controls, HEK 293 cells (lane 3) were immunoprecipitated with *anti*-HA 101R antibody, subjected to SDS–PAGE/Western blotting, followed by screening with the *anti*-HA 3F10 peroxidase-conjugated antibody and chemiluminescence detection. The relative positions of the molecular weight markers (kDa) are indicated to the left and right of panels (a) and (c), respectively. The arrow to the left of the panels indicates the position of the phosphorylated TPβ receptor. These data are representative of three independent experiments.

109203X impaired TPα phosphorylation in response to both ligands. On the other hand, neither 17 phenyl trinor PGE_2 nor $PGF_{2\alpha}$ increased the level phosphorylation of $TP\alpha^{T337A}$. Taken together, these data confirm that TPα is subject to EP_1- and FP-mediated desensitization through a GF 109203X-sensitive, PKC mechanism, and establish that Thr^{337}, located within the unique C-tail of TPα, represents the target site for both 17 phenyl trinor PGE_2 and $PGF_{2\alpha}$-induced phosphorylation.

In terms of EP_1- and FP-mediated desensitization of TPβ signalling, due to the abundance of Ser/Thr residues representing potential phospho-targets, deletion mutagenesis was initially used to generate the truncated variant $TP\beta^{\Delta367}$ devoid of those residues distal to Ile^{367}. Pre-stimulation of $TP\beta^{\Delta367}$ with either 17 phenyl trinor PGE_2 or $PGF_{2\alpha}$ did not significantly impair U46619-mediated $[Ca^{2+}]_i$ mobilization, indicating that the target site for both EP_1- and FP-mediated desensitization of TPβ signalling is located distal to Ile^{367}. Further sequence analysis identified two putative PKC consensus phosphorylation sites distal to Ile^{367} within TPβ (EPP$\underline{T}^{399}$GKAL$\underline{S}^{404}$RKD), where Thr^{399} and Ser^{404} represent the putative phospho-targets. Hence, Thr^{399} and Ser^{404} were mutated both collectively or individually to generate the variants $TP\beta^{T399A,S404A}$, $TP\beta^{T399A}$ and $TP\beta^{S404A}$. Stimulation of HEK.$TP\beta^{T399A,S404A}$ cells with either 17 phenyl trinor PGE_2 or $PGF_{2\alpha}$ did not desensitize U46619-mediated $[Ca^{2+}]_i$ mobilization, indicating that either Thr^{399} or Ser^{404} or both represent the target site(s) for both EP_1- and FP-mediated desensitization of TPβ signalling. While 17 phenyl trinor PGE_2 or PGF_2 had no effect on U46619-mediated $[Ca^{2+}]_i$ mobilization by $TP\beta^{T399A}$, both ligands significantly desensitized signalling by $TP\beta^{S404A}$. These data indicate that Thr^{399}, but not Ser^{404}, represents a target site for EP_1- and FP-mediated desensitization of TPβ signalling. Moreover, while both 17 phenyl trinor PGE_2 and $PGF_{2\alpha}$ each reduced U46619-mediated IP_3 generation by TPβ and $TP\beta^{S404A}$ (data not shown), neither ligand affected U46619-mediated IP_3 generation by $TP\beta^{T399A}$ or $TP\beta^{T399A,S404A}$ (data not shown). Whole-cell phosphorylation assays established that both 17 phenyl trinor PGE_2 or $PGF_{2\alpha}$ increased the level of TPβ phosphorylation, while the PKC inhibitor impaired both EP_1- and FP-mediated TPβ phosphorylation in response to either ligand. On the other hand, neither 17 phenyl trinor PGE_2 nor $PGF_{2\alpha}$ increased the level phosphorylation of $TP\beta^{T377A}$. Thus, taken together, these data confirm that TPβ is subject to EP_1- and FP-mediated desensitization through a GF 109203X-sensitive, PKC mechanism, and establish that Thr^{399}, located within the unique C-tail of TPβ, represents the target site for both 17 phenyl trinor PGE_2 and $PGF_{2\alpha}$ desensitization.

Thus, in this study, we have established that the TPα and TPβ isoforms of the human TP are subject to desensitization/intermolecular cross-talk mediated through the EP_1 and FP agonists, and show that this occurred by PKC phosphorylation at sites unique to the individual TP isoforms, pointing to further differences in the regulation of responses to TPα and TPβ. Intermolecular cross-talk has been extensively demonstrated between different GPCRs and their intracellular signalling pathways (Morris *et al*., 1991; Maggio *et al*., 1993; Chuang *et al*., 1996; Ozaki *et al*., 1997; Sulakhe *et al*., 1997; Selbie & Hill, 1998) and between GPCRs and members of the tyrosine kinase receptor family; for example, Chuang *et al*. (1996) and Selbie & Hill (1998). While such cross-talk provides potential regulatory mechanisms for the coordination and control of signalling events between different receptors, such as between the TP(s) and other receptor whose activities may impinge upon each other, such mechanisms are not necessarily predictable. For example, in A7r5 vascular smooth muscle cells transiently transfected with the TPα receptor, stimulation with the TXA_2 mimetic I-BOP leads to activation of the mitogen-activated protein kinase (MAPK) cascade with concomitant tyrosine phosphorylation of not only phosphoinositide 3-kinase, but also of TPα itself (Morinelli *et al*., 1997). As stated, TPα, but not TPβ, is subject to prostacyclin/

PGI_2-induced desensitization mediated through direct PKA phosphorylation of TPα at Ser^{329}, thereby revealing the important physiologic differences between the TP isoforms within the vasculature (Walsh *et al*., 2000). Similarly, in another study, Wang *et al*. (1998) identified the human platelet TP(s) as substrate(s) for cGMP-dependent protein kinase G (PKG) and proposed that direct TP phosphorylation by PKG may provide a mechanism for the inhibitory effects of the vasodilatory autocoid nitric oxide (NO) on TP responses within the vasculature. It has been recently established that, similar to that which occurs with prostacyclin, TPα but not TPβ undergoes NO-induced desensitization of signalling through a PKG mechanism involving direct phosphorylation of TPα at Ser^{331} within its C-tail domain (Reid & Kinsella, 2003). Moreover, these studies also clearly demonstrated that TPα undergoes both NO- and prostacyclin-mediated desensitization that occurs through entirely *independent mechanisms* involving direct PKG phosphorylation of Ser^{331}, in response to NO, and PKA phosphorylation of Ser^{329}, in response to prostacyclin, within the unique C-tail domain of TPα. On the other hand, signalling by TPβ is unaffected by either NO or prostacyclin (Walsh *et al*., 2000; Reid & Kinsella, 2003). Moreover, the PKC-dependent, EP_1/FP receptor-mediated regulation of the TP isoforms reported herein is not predictable simply due to coincident activation of PKC associated with EP_1/FP receptor/PLC coupling. For example, we and others (Thomas *et al*., 1995; Habib *et al*., 1997; 1999; Kinsella *et al*., 1997) have established that signalling by the TP receptors expressed in platelets or HEK 293 cells is not subject to desensitization due to thrombin activation of the PLC/PKC system and *vice versa*.

While EP_1, FP and TP receptors are each broadly classified as members of the contractile subgroup of prostanoid receptors (Narumiya *et al*., 1999), functionally they are primarily associated with distinct physiologic processes and each exhibit distinct patterns of expression (Narumiya *et al*., 1999; Sugimoto *et al*., 2000). Consistent with the latter, mice deficient in each of these receptors display unique characteristic phenotypes including a reduction in carcinogen-induced colorectal cancer in EP_1-deficient mice (Ushikubi *et al*., 1998; Watanabe *et al*., 1999; Sugimoto *et al*., 2000), loss of parturition affecting both ovulation and fertilization in FP-deficient mice (Sugimoto *et al*., 1997; Hizaki *et al*., 1999; Kennedy *et al*., 1999) and increased bleeding tendency associated with TP-deficient mice (Thomas *et al*., 1998). While EP_1, FP and TP receptors are also abundantly expressed in the kidney (Sugimoto *et al*., 2000) and they are each reported to mediate efficient contraction of renal vascular SM and mesangial cells through Ca^{2+}-dependent mechanisms (Mene *et al*., 1989), their role in renal function as garnered from mouse knockout studies remains to be clearly established. While the precise intrarenal distribution of the FP has not yet been reported, *in situ* hybridization has localized the EP_1 largely to the cortical collecting duct (Hebert *et al*., 1991; Hebert, 1994). Similarly, *in situ* hybridization studies in the rat confirmed the abundant expression of the TP within the glomerulus, arterioles and epithelium lining the urinary pelvis and an absence of/reduced expression in the proximal tubule, cortical thick limb or the collecting duct (Abe *et al*., 1995). However, despite this knowledge, the relative roles of the individual EP_1, FP and TP prostanoid receptors within the kidney remain largely unknown and the significance of two TP isoforms, namely TPα and TPβ, to renal function in humans remains to be investigated. The study of the intermolecular cross-talk by the latter prostanoid receptors and their ligands on TPα/TPβ signalling reported herein sheds some novel insight on how the TP isoforms are regulated, such as within renal mesangial cells.

This research was supported by grants to BTK from the Wellcome Trust, Enterprise Ireland and The Health Research Board (Ireland).

References

ABE, T., TAKEUCHI, K., TAKAHASHI, N., TSUTSUMI, E., TANIYAMA, Y. & ABE, K. (1995). Rat kidney thromboxane receptor: molecular cloning, signal transduction, and intrarenal expression localization. *J. Clin. Invest.,* **96,** 657–664.

ABRAMOVITZ, M., BOIE, Y., NGUYEN, T., RUSHMORE, T.H., BAYNE, M.A., METTERS, K.M., SLIPETZ, D.M. & GRYGORCZYK, R. (1994). Cloning and expression of a cDNA for the human prostanoid FP receptor. *J. Biol. Chem.,* **269,** 2632–2636.

ARMSTRONG, R.A. (1996). Platelet prostanoid receptors. *Pharmacol. Ther.,* **72,** 171–191.

BADR, K.F. (1992). Sepsis-associated renal vasoconstriction: potential targets for future therapy. *Am. J. Kidney Dis.,* **20,** 207–213.

BLOM, N., KREEGIPUU, A. & BRUNAK, S. (1998). PhosphoBase: a database of phosphorylation sites. *Nucleic Acids Res.,* **26,** 382–386.

BRADFORD, M.M. (1976). A rapid and sensitive method for the quantitation of microgram quantities of protein utilizing the principle of protein–dye binding. *Anal. Biochem.,* **72,** 248–254.

BREYER, M.D. (1998). Prostaglandin receptors in the kidney: a new route for intervention? *Exp. Nephrol.,* **6,** 180–188.

BUNCE, K.T., CLAYTON, N.M., COLEMAN, R.A., COLLINGTON, E.W., FINCH, H., HUMPHRAY, J.M., HUMPHREY, P.P., REEVES, J.J., SHELDRICK, R.L. & STABLES, R. (1991). GR63799X – a novel prostanoid with selectivity for EP3 receptors. *Adv. Prostagland. Thromboxane Leukotr. Res.,* **21A,** 379–382.

CHUANG, T.T., IACOVELLI, L., SALLESE, M. & DE BLASI, A. (1996). G protein-coupled receptors: heterologous regulation of homologous desensitization and its implications. *Trends Pharmacol. Sci.,* **17,** 416–421.

COLEMAN, R.A., SMITH, W.L. & NARUMIYA, S. (1994). International Union of Pharmacology classification of prostanoid receptors: properties, distribution, and structure of the receptors and their subtypes. *Pharmacol. Rev.,* **46,** 205–229.

COYLE, A.T., MIGGIN, S.M. & KINSELLA, B.T. (2002). Characterization of the 5′ untranslated region of alpha and beta isoforms of the human thromboxane A2 receptor (TP). Differential promoter utilization by the TP isoforms. *Eur. J. Biochem.,* **269,** 4058–4073.

DERUBERTIS, F.R. & CRAVEN, P.A. (1993). Eicosanoids in the pathogenesis of the functional and structural alterations of the kidney in diabetes. *Am. J. Kidney Dis.,* **22,** 727–735.

FENNEKOHL, A., SCHIEFERDECKER, H.L., JUNGERMANN, K. & PUSCHEL, G.P. (1999). Differential expression of prostanoid receptors in hepatocytes, Kupffer cells, sinusoidal endothelial cells and stellate cells of rat liver. *J. Hepatol.,* **30,** 38–47.

FIELD, J., NIKAWA, J., BROEK, D., MACDONALD, B., RODGERS, L., WILSON, I.A., LERNER, R.A. & WIGLER, M. (1988). Purification of a RAS-responsive adenylyl cyclase complex from *Saccharomyces cerevisiae* by use of an epitope addition method. *Mol. Cell. Biol.,* **8,** 2159–2165.

FOLEY, J.F., KELLEY, L.P. & KINSELLA, B.T. (2001). Prostaglandin D(2) receptor-mediated desensitization of the alpha isoform of the human thromboxane A(2) receptor. *Biochem. Pharmacol.,* **62,** 229–239.

FUNK, C.D., FURCI, L., FITZGERALD, G.A., GRYGORCZYK, R., ROCHETTE, C., BAYNE, M.A., ABRAMOVITZ, M., ADAM, M. & METTERS, K.M. (1993). Cloning and expression of a cDNA for the human prostaglandin E receptor EP1 subtype. *J. Biol. Chem.,* **268,** 26767–26772.

GODFREY, P. (1992). Inositol lipids and phosphates. In: *Signal Transduction: A Practical Approach,* ed. Milligan, G. Oxford: IRL Press.

GORMAN, C.M., GIES, D.R. & MSCRAY, G. (1990). Transient production of proteins using an adenovirus transformed cell line. *DNA Prot. Eng. Tech.,* **2,** 3–10.

GRYNKIEWICZ, G., POENIE, M. & TSIEN, R.Y. (1985). A new generation of Ca^{2+} indicators with greatly improved fluorescence properties. *J. Biol. Chem.,* **260,** 3440–3450.

HABIB, A., FITZGERALD, G.A. & MACLOUF, J. (1999). Phosphorylation of the thromboxane receptor alpha, the predominant isoform expressed in human platelets. *J. Biol. Chem.,* **274,** 2645–2651.

HABIB, A., VEZZA, R., CREMINON, C., MACLOUF, J. & FITZGERALD, G.A. (1997). Rapid, agonist-dependent phosphorylation *in vivo* of human thromboxane receptor isoforms. Minimal involvement of protein kinase C. *J. Biol. Chem.,* **272,** 7191–7200.

HAYES, J.S., LAWLER, O.A., WALSH, M.T. & KINSELLA, B.T. (1999). The prostacyclin receptor is isoprenylated. Isoprenylation is required for efficient receptor–effector coupling. *J. Biol. Chem.,* **274,** 23707–23718.

HEBERT, R.L. (1994). Cellular signalling of PGE2 and its selective receptor analogue sulprostone in rabbit cortical collecting duct. *Prostagland. Leukotr. Essent. Fatty Acids,* **51,** 147–155.

HEBERT, R.L., JACOBSON, H.R. & BREYER, M.D. (1991). Prostaglandin E2 inhibits sodium transport in rabbit cortical collecting duct by increasing intracellular calcium. *J. Clin. Invest.,* **87,** 1992–1998.

HIRATA, M., HAYASHI, Y., USHIKUBI, F., YOKOTA, Y., KAGEYAMA, R., NAKANISHI, S. & NARUMIYA, S. (1991). Cloning and expression of cDNA for a human thromboxane A2 receptor. *Nature,* **349,** 617–620.

HIRATA, T., USHIKUBI, F., KAKIZUKA, A., OKUMA, M. & NARUMIYA, S. (1996). Two thromboxane A2 receptor isoforms in human platelets. Opposite coupling to adenylyl cyclase with different sensitivity to Arg60 to Leu mutation. *J. Clin. Invest.,* **97,** 949–956.

HIZAKI, H., SEGI, E., SUGIMOTO, Y., HIROSE, M., SAJI, T., USHIKUBI, F., MATSUOKA, T., NODA, Y., TANAKA, T., YOSHIDA, N., NARUMIYA, S. & ICHIKAWA, A. (1999). Abortive expansion of the cumulus and impaired fertility in mice lacking the prostaglandin E receptor subtype EP(2). *Proc. Natl. Acad. Sci. U.S.A.,* **96,** 10501–10506.

INOUE, H., TSUJISAWA, T., FUKUIZUMI, T., KAWAGISHI, S. & UCHIYAMA, C. (1999). SC-19220, a prostaglandin E2 antagonist, inhibits osteoclast formation by 1,25-dihydroxyvitamin D3 in cell cultures. *J. Endocrinol.,* **161,** 231–236.

KENNEDY, C.R., ZHANG, Y., BRANDON, S., GUAN, Y., COFFEE, K., FUNK, C.D., MAGNUSON, M.A., OATES, J.A., BREYER, M.D. & BREYER, R.M. (1999). Salt-sensitive hypertension and reduced fertility in mice lacking the prostaglandin EP2 receptor. *Nat. Med.,* **5,** 217–220.

KINSELLA, B.T. (2001). Thromboxane A2 signalling in humans: a 'Tail' of two receptors. *Biochem. Soc. Trans.,* **29,** 641–654.

KINSELLA, B.T., O'MAHONY, D.J. & FITZGERALD, G.A. (1997). The human thromboxane A2 receptor alpha isoform (TP alpha) functionally couples to the G proteins Gq and G11 *in vivo* and is activated by the isoprostane 8-epi prostaglandin F2 alpha. *J. Pharmacol. Exp. Ther.,* **281,** 957–964.

KIRIYAMA, M., USHIKUBI, F., KOBAYASHI, T., HIRATA, M., SUGIMOTO, Y. & NARUMIYA, S. (1997). Ligand binding specificities of the eight types and subtypes of the mouse prostanoid receptors expressed in Chinese hamster ovary cells. *Br. J. Pharmacol.,* **122,** 217–224.

MAGGIO, R., VOGEL, Z. & WESS, J. (1993). Coexpression studies with mutant muscarinic/adrenergic receptors provide evidence for intermolecular "cross-talk" between G-protein-linked receptors. *Proc. Natl. Acad. Sci. U.S.A.,* **90,** 3103–3107.

MENE, P., SIMONSON, M.S. & DUNN, M.J. (1989). Physiology of the mesangial cell. *Physiol. Rev.,* **69,** 1347–1424.

MIGGIN, S.M. & KINSELLA, B.T. (1998). Expression and tissue distribution of the mRNAs encoding the human thromboxane A2 receptor (TP) alpha and beta isoforms. *Biochim. Biophys. Acta,* **1425,** 543–559.

MORINELLI, T.A., FINLEY, E.L., JAFFA, A.A., KURTZ, D.T. & ULLIAN, M.E. (1997). Tyrosine phosphorylation of phosphatidylinositol 3-kinase and of the thromboxane A2 (TXA2) receptor by the TXA2 mimetic I-BOP in A7r5 cells. *Biochem. Pharmacol.,* **53,** 1823–1832.

MORRIS, G.M., HADCOCK, J.R. & MALBON, C.C. (1991). Cross-regulation between G-protein-coupled receptors. Activation of beta 2-adrenergic receptors increases alpha 1-adrenergic receptor mRNA levels. *J. Biol. Chem.,* **266,** 2233–2238.

NARUMIYA, S., SUGIMOTO, Y. & USHIKUBI, F. (1999). Prostanoid receptors: structures, properties, and functions. *Physiol. Rev.,* **79,** 1193–1226.

OZAKI, S., OHWAKI, K., IHARA, M., ISHIKAWA, K. & YANO, M. (1997). Coexpression studies with endothelin receptor subtypes indicate the existence of intracellular cross-talk between ET(A) and ET(B) receptors. *J. Biochem. (Tokyo),* **121,** 440–447.

PARENT, J.L., LABRECQUE, P., DRISS ROCHDI, M. & BENOVIC, J.L. (2001). Role of the differentially spliced carboxyl terminus in thromboxane A2 receptor trafficking: identification of a distinct motif for tonic internalization. *J. Biol. Chem.,* **276,** 7079–7085.

PARENT, J.L., LABRECQUE, P., ORSINI, M.J. & BENOVIC, J.L. (1999). Internalization of the TXA2 receptor alpha and beta isoforms. Role of the differentially spliced COOH terminus in agonist-promoted receptor internalization. *J. Biol. Chem.,* **274,** 8941–8948.

RAYCHOWDHURY, M.K., YUKAWA, M., COLLINS, L.J., MCGRAIL, S.H., KENT, K.C. & WARE, J.A. (1994). Alternative splicing produces a divergent cytoplasmic tail in the human endothelial thromboxane A2 receptor. *J. Biol. Chem.,* **269,** 19256–19261.

REID, H.M. & KINSELLA, B.T. (2003). The alpha, but not the beta, isoform of the human thromboxane A2 receptor is a target for nitric oxide-mediated desensitization: independent modulation of TP alpha signaling by nitric oxide and prostacyclin. *J. Biol. Chem.,* **278,** 51190–51202.

SELBIE, L.A. & HILL, S.J. (1998). G protein-coupled-receptor cross-talk: the fine-tuning of multiple receptor-signalling pathways. *Trends Pharmacol. Sci.,* **19,** 87–93.

SMITH, G.C., COLEMAN, R.A. & MCGRATH, J.C. (1994). Characterization of dilator prostanoid receptors in the fetal rabbit ductus arteriosus. *J. Pharmacol. Exp. Ther.,* **271,** 390–396.

SPURNEY, R.F., ONORATO, J.J., ALBERS, F.J. & COFFMAN, T.M. (1993a). Thromboxane binding and signal transduction in rat glomerular mesangial cells. *Am. J. Physiol.,* **264,** F292–F299.

SPURNEY, R.F., ONORATO, J.J., RUIZ, P., PISETSKY, D.S. & COFFMAN, T.M. (1993b). Characterization of glomerular thromboxane receptors in murine lupus nephritis. *J. Pharmacol. Exp. Ther.,* **264,** 584–590.

SUGIMOTO, Y., NARUMIYA, S. & ICHIKAWA, A. (2000). Distribution and function of prostanoid receptors: studies from knockout mice. *Prog. Lipid Res.,* **39,** 289–314.

SUGIMOTO, Y., YAMASAKI, A., SEGI, E., TSUBOI, K., AZE, Y., NISHIMURA, T., OIDA, H., YOSHIDA, N., TANAKA, T., KATSUYAMA, M., HASUMOTO, K., MURATA, T., HIRATA, M., USHIKUBI, F., NEGISHI, M., ICHIKAWA, A. & NARUMIYA, S. (1997). Failure of parturition in mice lacking the prostaglandin F receptor. *Science,* **277,** 681–683.

SULAKHE, P.V., VO, X.T. & MAINRA, R.R. (1997). Differential nature of cross-talk among three G-coupled receptors regulating adenylyl cyclase in rat cardiomyocytes chronically exposed to receptor agonists. *Mol. Cell. Biochem.,* **176,** 75–82.

TALPAIN, E., ARMSTRONG, R.A., COLEMAN, R.A. & VARDEY, C.J. (1995). Characterization of the PGE receptor subtype mediating inhibition of superoxide production in human neutrophils. *Br. J. Pharmacol.,* **114,** 1459–1465.

THOMAS, C.P., DUNN, M.J. & MATTERA, R. (1995). Ca^{2+} signalling in K562 human erythroleukaemia cells: effect of dimethyl sulphoxide and role of G-proteins in thrombin- and thromboxane A2-activated pathways. *Biochem. J.,* **312** (Part 1), 151–158.

THOMAS, D.W., MANNON, R.B., MANNON, P.J., LATOUR, A., OLIVER, J.A., HOFFMAN, M., SMITHIES, O., KOLLER, B.H. & COFFMAN, T.M. (1998). Coagulation defects and altered hemodynamic responses in mice lacking receptors for thromboxane A2. *J. Clin. Invest.,* **102,** 1994–2001.

USHIKUBI, F., SEGI, E., SUGIMOTO, Y., MURATA, T., MATSUOKA, T., KOBAYASHI, T., HIZAKI, H., TUBOI, K., KATSUYAMA, M., ICHIKAWA, A., TANAKA, T., YOSHIDA, N. & NARUMIYA, S. (1998). Impaired febrile response in mice lacking the prostaglandin E receptor subtype EP3. *Nature,* **395,** 281–284.

VAN DER VUURST, H., VAN WILLIGEN, G., VAN SPRONSEN, A., HENDRIKS, M., DONATH, J. & AKKERMAN, J.W. (1997). Signal transduction through trimeric G proteins in megakaryoblastic cell lines. *Arterioscler. Thromb. Vasc. Biol.,* **17,** 1830–1836.

VEZZA, R., HABIB, A. & FITZGERALD, G.A. (1999). Differential signaling by the thromboxane receptor isoforms *via* the novel GTP-binding protein, Gh. *J. Biol. Chem.,* **274,** 12774–12779.

WALSH, M.T., FOLEY, J.F. & KINSELLA, B.T. (2000). Investigation of the role of the carboxyl-terminal tails of the alpha and beta isoforms of the human thromboxane A(2) receptor (TP) in mediating receptor : effector coupling. *Biochim. Biophys. Acta,* **1496,** 164–182.

WALSH, M.T., FOLEY, J.F. & KINSELLA, B.T. (1998). Characterization of the role of N-linked glycosylation on the cell signaling and expression of the human thromboxane A2 receptor alpha and beta isoforms. *J. Pharmacol. Exp. Ther.,* **286,** 1026–1036.

WALSH, M.T., FOLEY, J.F. & KINSELLA, B.T. (2000). The alpha, but not the beta, isoform of the human thromboxane A2 receptor is a target for prostacyclin-mediated desensitization. *J. Biol. Chem.,* **275,** 20412–20423.

WALSH, M.T. & KINSELLA, B.T. (2000). Regulation of the human prostanoid TPalpha and TPbeta receptor isoforms mediated through activation of the EP(1) and IP receptors. *Br. J. Pharmacol.,* **131,** 601–609.

WALT, R.P. (1992). Misoprostol for the treatment of peptic ulcer and antiinflammatory-drug-induced gastroduodenal ulceration. *N. Engl. J. Med.,* **327,** 1575–1580.

WANG, G.R., ZHU, Y., HALUSHKA, P.V., LINCOLN, T.M. & MENDELSOHN, M.E. (1998). Mechanism of platelet inhibition by nitric oxide: *in vivo* phosphorylation of thromboxane receptor by cyclic GMP-dependent protein kinase. *Proc. Natl. Acad. Sci. U.S.A.,* **95,** 4888–4893.

WATABE, A., SUGIMOTO, Y., HONDA, A., IRIE, A., NAMBA, T., NEGISHI, M., ITO, S., NARUMIYA, S. & ICHIKAWA, A. (1993). Cloning and expression of cDNA for a mouse EP1 subtype of prostaglandin E receptor. *J. Biol. Chem.,* **268,** 20175–20178.

WATANABE, K., KAWAMORI, T., NAKATSUGI, S., OHTA, T., OHUCHIDA, S., YAMAMOTO, H., MARUYAMA, T., KONDO, K., USHIKUBI, F., NARUMIYA, S., SUGIMURA, T. & WAKABAYASHI, K. (1999). Role of the prostaglandin E receptor subtype EP1 in colon carcinogenesis. *Cancer Res.,* **59,** 5093–5096.

WILKES, B.M., SOLOMON, J., MAITA, M. & MENTO, P.F. (1989). Characterization of glomerular thromboxane receptor sites in the rat. *Am. J. Physiol.,* **256,** F1111–F1116.

WISE, H. & JONES, R.L. (1996). Focus on prostacyclin and its novel mimetics. *Trends Pharmacol. Sci.,* **17,** 17–21.

YAMAMOTO, S., YAN, F., ZHOU, H. & TAI, H.H. (2001). Serine 331 is the major site of receptor phosphorylation induced by agents that activate protein kinase G in HEK 293 cells overexpressing thromboxane receptor alpha. *Arch. Biochem. Biophys.,* **393,** 97–105.

(Received November 3, 2003
Revised January 5, 2004
Accepted January 13, 2004)